THE EFFECT OF PULSE WIDTH MODULATED SIGNALS ON TWO-PHASE SERVOMOTORS

E. W. HAYS
AND
W. W. LAKE

THE EFFECT OF PULSE WIDTH MODULATED SIGNALS ON TWO-PHASE SERVOMOTORS

* * * * * * * * * * * * *

Estel W. Hays

and

Walter W. Lake

THE EFFECT OF PULSE WIDTH MODULATED SIGNALS

ON

TWO-PHASE SERVOMOTORS

by

Estel Wilbur HAYS

Lieutenant, United States Navy

and

Walter Williams LAKE

Lieutenant, United States Navy

Submitted in partial fulfillment of
the requirements for the degree of

MASTER OF SCIENCE

IN

ELECTRICAL ENGINEERING

United States Naval Postgraduate School
Monterey, California

1 9 5 9

THE EFFECT OF PULSE WIDTH MODULATED SIGNALS ON TWO-PHASE SERVOMOTORS

by

E. W. Hays and W. W. Lake

This work is accepted as fulfilling
the thesis requirements for the degree of

MASTER OF SCIENCE

IN

ELECTRICAL ENGINEERING

from the

United States Naval Postgraduate School

ABSTRACT

This investigation was undertaken to determine the feasibility of operating a two-phase servomotor using pulse width modulated control voltages. This study has shown such operation of motors to be both feasible and practical in most control systems. The motor torque is slightly reduced when both motor fields are pulsed with small error signals, and unchanged for operation with only the control field pulsed. Heating effects were found to be small, and either increased or decreased from that of a motor with normal sinusoidal excitation, dependent on motor usage.

This investigation was conducted by Lt Hays and Lt. Lake at the United States Naval Postgraduate School and Dalmo Victor Company of Belmont, California during 1959. This was a primary investigation to a larger project of developing a pulse width modulated servosystem, utilizing a switching transistor amplifier.

ACKNOWLEDGEMENT

The authors wish to express their appreciation to Mr. Herman Chanowitz and Mr. Robert P. McIntosh of Dalmo Victor Company for their counsel and assistance given during this investigation, to the personnel of Dalmo Victor Company for their cooperation with this investigation, and to Dr. Marvin P. Pastel for assistance as faculty advisor.

TABLE OF CONTENTS

LIST OF ILLUSTRATIONS

TABLE OF SYMBOLS AND ABREVIATIONS

Symbol	Description
a	Width of pulse
$a_0, a_1, a_2, \cdots$	Coefficients for Fourier series
A	Amplitude of pulses
$b_1, b_2, \cdots$	Coefficients for Fourier series
B	Temperature
B_o	Reference temperature
C	Centigrade
cm	Centimeter
cycle	Cycles per second, frequency of sinusoid waveform
d	Diameter of rotor
D	Distance between suspension points
d.c.	Direct current
f(t)	Function of time
G(jw)	Transfer function
gm	Gram
I	Current
I_m	Current for airgap and core loss
I_r	Current through rotor
I_s	Current through stator winding
in	Inch
j	Imaginary number
J	Rotor polar moment of Inertia
K	Gain of servomotor

Symbol	Description
ℓ	Length of string
n	An integer
N	Effective field winding turns
N_s	Synchronous speed of motor
oz	Ounce
P	Power
P_{rt}	Total power to rotor
Q	Ratio of stall torque to driving torque
r, R	Resistance
rad	Radians
rev	Revolutions
RMS	Root mean square
rpm	Revolutions per minute
s	Rotor slip
sec	Second
t	Time
T	Period of oscillation, timeof one cycle
T	Torque
T_{st}	Stall Torque
V	Voltage
w	Angular velocity, frequency (rad per sec)
W	Weight of rotor
x	Inductive reactance
α	Temperature coefficient of resistance
δ	Pulse width, fraction of a square wave

Symbol	Description
θ	Angle
θ_c	Motor shaft output
τ	Time constant

CHAPTER I

INTRODUCTION

In modern missile and aircraft designs the servo systems, specifically antenna drive and aerodynamic surface control systems, are often located in small isolated compartments. The conditions caused by space and weight considerations do not provide for temperature control or heat dissapation. Under such conditions the heat produced by a conventional vacuum tube power amplifier in a servo system may be unacceptable. A large amount of heat is produced by such amplifiers because of filament heating required in vacuum tubes, and the heat loss due to the inherent inefficiency of a vacuum tube amplifier, where waste power appears as temperature rise.

A linear transistorized amplifier would eliminate the filament heating and reduce the amount of space required. Even so, transistors operating in the linear characteristics range are inefficient, with a power loss as heat. One possible solution to the problem is to use transistors operating in the switching mode (1)*. In this mode of operation a transistor is operated either in a fully conducting, or a fully cut-off condition, passing through the intermediate linear characteristics

* Indicates reference, numbered as listed in BIBLIOGRAPHY

range very rapidly. In this way high power can be passed by small transistors with very little heat generation. This is the situation since the transistor is either fully off with no current conducted, or is fully conducting, presenting a very small resistance to current flow. Under this condition there is little power loss to generate a temperature rise.

One method of utilizing a switching transistor power amplifier in a servo system is a method envisioned by Mr. Herman Chanowitz of Dalmo Victor Company. This method entails the amplification of pulses causing rapid transition from fully conducting to completely off states for the transistors. This may be accomplished by generating pulses to drive a two-phase servomotor, the pulse width being proportional to the error signal. A possible simplified block diagram is:

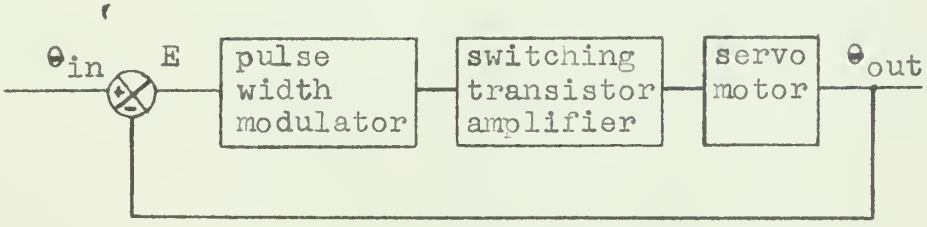

Prior to development of the pulse width modulator and switching transistor amplifier it was necessary to know the characteristics of the two-phase electrical servomotor operating on pulses. The investigation of the effect of pulsed excitation on the motor was undertaken as a preliminary part of the development of the servo system, and is

the subject of this report. The immediate objectives were to determine the effects of the harmonics present in the variable width pulses as pertained to torque-speed response and temperature effects. This investigation was limited to one servomotor considered to have characteristics representative of the newer, small, high-torque servomotors.

The investigation was divided roughly into three parts. First: obtaining the characteristics and torque-speed response for balanced and unbalanced normal sinusoidal excitation. Second; predicting mathematically the effect of pulse excitation on the motor response. Third; the actual testing of the motor using pulse signals on one and/or both motor fields.

The test results in this investigation tend to verify the mathematical predictions pertaining to the response characteristics of the motor.

CHAPTER II

PRELIMINARY INVESTIGATION

The servomotor used in this investigation was a 115 volt, 400 cycle, two-phase servomotor, built by American Electronics Incorporated, Culver City, California. This motor was built to meet specifications originated by Dalmo Victor Company. The specific motor tested was model number SM18AJ26T, serial 01045.

Since this was a new motor constructed to certain specifications, there were no known motor characteristics available. Also, characteristics under both balanced and unbalanced operating conditions were desired. For these reasons it was necessary to conduct various tests on the motor under normal sine wave operation prior to commencing any studies for pulse excitation of the motor.

The tests conducted include torque-speed measurements, temperature-speed measurements, velocity response, transient response, measurement of rotor moment of inertia, and static current frequency response. These tests were conducted using standard test procedures to obtain motor characteristics and to assist in construction of an equivalent circuit.

The torque-speed curves were obtained using a dynamometer employing a d.c. brake to vary the torque loading and motor speed. For unbalanced operating conditions the

reference phase of the motor was connected to a fixed 115 volt, 400 cycle source, and the control phase was connected to a variable voltage, 400 cycle source. These standard torque-speed curves are shown as Fig. 1. Fig. 2 shows the torque-speed curves for balanced conditions, where both motor fields were operated at the same 400 cycle voltage level, with the two field voltages being in quadrature.

Stall torque was measured for balanced conditions of excitation at 400 and 1200 cycles. The values of stall torque at various control voltages for both 400 and 1200 cycles are shown in Fig. 3. This figure indicates that the torque due to a 1200 cycle voltage is quite small in comparison to the torque produced by a 400 cycle voltage of equal magnitude.

During the torque-speed tests, temperatures were recorded for the motor case, windings, and shaft bearing face. The case and bearing face temperatures were measured by means of a thermocouple. The winding temperature was obtained by measuring the winding resistance using a resistance bridge, and using the relationship:

$$B = B_o - \frac{R_{B_o} - R_B}{R_{B_o} \alpha} \qquad (8)$$

where: B = unknown temperature in degrees centigrade

R_B = resistance at B

B_o = 25 C, reference temperature

R_{B_o} = resistance at B_o , 21.79 ohms

α = temperature coefficient of resistance
0.00335 ohms per degree centigrade

Fig. 4 shows the variation of these temperatures with torque loading, and the relationship between these temperatures for a typical run. The bearing face temperature was lower than the case temperature because of heat dissapation away from this face into the motor mounting plate.

Fig. 5 shows the static winding current values for each winding of the motor. Each winding exhibited the same static current characteristics, measured by applying a voltage to the winding, and measuring current with the rotor removed. These measurements, taken at several voltage levels over a range of frequencies, show the variation of winding current with frequency.

The frequency response was obtained from the observed velocity response, plus values from a computed transfer function. The velocity response was obtained using a 400 cycle tachometer coupled to the motor shaft. An input signal to the control phase was modulated at various frequencies by a dynamic servo analyzer. Measurements were made using an oscilloscope, comparing phase by the angular displacement of the null, and amplitude by relative amplitude of signals as shown in Fig. 7. Tests were limited to voltages below the 60 volt level to prevent velocity saturation of the test motor. The velocity response for a control voltage of 40 RMS volts is shown in Fig. 8. From these curves an approximate time constant of τ =

0.0323 seconds for the motor was obtained as the reciprocal of the -45 degree phase angle frequency. This closely agrees with the corner frequency of the magnitude curve.

The value of gain (K) used in plotting the frequency response was the value from the calculated transfer function for the approximated linear second-order motor:

$$KG(jw) = \frac{K}{jw(jw\tau + 1)} \qquad (2)$$

The transfer function was determined using values from the 40 volt curve of Fig. 1 and the equation:

$$\frac{\theta_c}{V} = \frac{\frac{Q}{\partial T/\partial w}}{jw\left(jw \frac{J}{\partial T/\partial w} + 1 \right)} \qquad (2)$$

where: $Q = \frac{\text{stall torque}}{\text{driving voltage}} = \frac{2.1 \text{ (in. oz)}}{40 \text{ (volts)}}$

$= 0.0525 \frac{\text{in oz}}{\text{volt}}$

$\frac{\partial T}{\partial w}$ = slope of torque-speed curve

$= \frac{40}{10{,}000} = 2.395 \times 10^{-4} \frac{\text{in oz}}{\text{rpm}}$

J = polar moment of inertia

= 6.0 gm cm^2 (specifications)

The term $\frac{Q}{\partial T/\partial w}$ is the gain and equal to:

$$K = \frac{Q}{\partial T/\partial w} = \frac{0.0525}{2.395 \times 10^{-4}} = 219 \frac{\text{rpm}}{\text{volt}}$$

For determination of the time constant the expressions J and $\partial T/\partial w$ must be in dimensionly consistant units:

$$J = 6 \text{ gm cm}^2 \times \frac{1 \text{ sec}^2}{980.66 \text{ cm}} \times \frac{1 \text{ oz}}{28.35 \text{gm}} \times \frac{1 \text{ in}}{2.54 \text{cm}}$$

$$= 8.45 \times 10^{-5} \text{ in oz sec}^2$$

$$\frac{\partial T}{\partial w} = 2.395 \times 10^{-4} \frac{\text{in oz}}{\text{rpm}} \times \frac{1 \text{ rev}}{2\pi} \times \frac{60 \text{ sec}}{1 \text{ min}}$$

$$= 22.9 \times 10^{-4} \text{ in oz sec}$$

The term $\frac{J}{\partial T/\partial w}$ is the time constant of the motor and is equal to:

$$\tau = \frac{8.45 \times 10^{-5}}{22.9 \times 10^{-4}} = 0.0369 \text{ seconds}$$

This gives the transfer function:

$$\frac{\theta_c}{V} = \frac{219}{jw(0.0369jw + 1)}$$

Using this value of K and the two values for the time constant (experimental and computed) the Bode Diagrams were drawn as Fig. 9. The computed time constant of 36.9 milliseconds agrees with the time constant of 32.8 milliseconds found by the velocity response test for a 40 volt signal on the control field.

The transient response was observed by applying a step voltage to the motor and observing the output of the tachometer on an oscilloscope (TEKTRONIX 515). By measuring the time required for the transient to achieve 63 per cent of its final value, a motor time constant was obtained. For the 115 RMS volt control voltage a time constant of 24.0 milliseconds was measured. The transient response varied noticeably for several other values of control voltage, giving a range of time constants from 24.0 milliseconds

to 42.0 milliseconds at low voltage. This indicates a non-linear servomotor (3). The time constant for a control field voltage of 40 R.M.S volts was 37.5 milliseconds. This value checks closely with the time constants obtained by other methods.

The rotor moment of inertia, J, was checked by the Torsion Wire Pendulum Method (4) using two suspension wires. For this measurement the motor rotor was removed and suspended as shown:

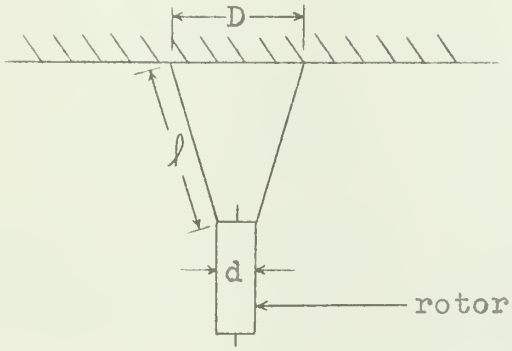

J was determined by twisting the rotor about its axis, releasing it, and recording the period of oscillation. J is obtained by the relation:

$$J = \frac{WDdT^2}{16\pi^2 \ell}$$

where W = weight of rotor, 0.0716 lbs.

D = distance between suspension points
= 2.89 inches

d = diameter of rotor, 0.48 inches

ℓ = length of each thread, 7.63 inches

T = period of oscillation, 0.28 seconds

The value obtained, $J = 7.24$ gm cm^2, was in fair agreement with the value of 6 gm cm^2 given by the motor specifications. The latter value was used for all calculations due to accuracy limitations of the experimental process used in measuring J.

An equivalent circuit of the motor was determined using values of Table I recorded during the torque-speed measurements. The equivalent circuit for each winding was determined as shown in Appendix A.

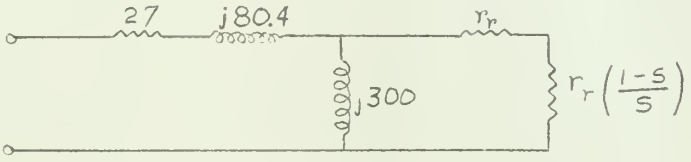

All parameters of the equivalent circuit were found to be nearly fixed in value except r_r, the reflected rotor resistance to the stator winding, which changed with variation in rotor speed and applied voltage as shown in Fig. 6.

The transfer function and the equivalent circuit of the motor were determined to make possible a mathematical prediction of the effect of pulse excitation. They will be used further in this investigation.

CHAPTER III

PREDICTION OF EFFECTS OF PULSE INPUT

3.1 Fourier Series for Pulse Train.

There are infinite possible Fourier series for any periodic waveform, depending on the zero reference selected, the units used, and other variables. In the specific case studied, that of flat topped, full wave, constant amplitude pulses, it was desired to derive an equation which would yield the amplitude of each harmonic component as a function of pulse width. It was found convenient to establish the zero reference and the basic parameters as shown:

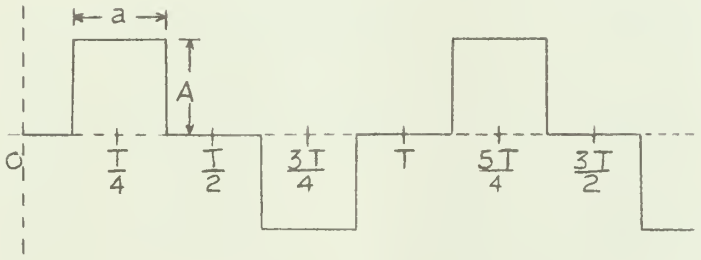

The general mathematical expression for the Fourier series is:

$$f(t) = a_{o/2} + a_1 \cos wt + a_2 \cos 2wt + a_3 \cos 3wt + \ldots$$
$$\ldots + b_1 \sin wt + b_2 \sin 2wt + b_3 \sin 3wt + \ldots.$$

where: a_o, a_1, b_1, a_2, b_2, etc. are numerical coefficients

w is the fundamental harmonic frequency in radians per second

The frequency, w, is related to the period T by

$$w = 2\pi / T$$

where T is the repetition period in seconds.

This general form can be simplified by noting that the wave form being studied is an odd function (5); therefore only sine terms will exist in the series. Thus the problem is reduced to finding b_1, b_2, b_3, etc. The formula for finding the necessary coefficients (b_n) is:

$$b_n = 2/T \int f(t) \left[\sin nwt\right] dt$$

In order to find this integral over the entire period, T, it is necessary to define the limits as follows:

from:		to		
	0	to	$\left(\frac{T}{4} - \frac{a}{2}\right)$	$f(t) = 0$
	$\left(\frac{T}{4} - \frac{a}{2}\right)$	to	$\left(\frac{T}{4} + \frac{a}{2}\right)$	$f(t) = A$
	$\left(\frac{T}{4} + \frac{a}{2}\right)$	to	$\left(\frac{3T}{4} - \frac{a}{2}\right)$	$f(t) = 0$
	$\left(\frac{3T}{4} - \frac{a}{2}\right)$	to	$\left(\frac{3T}{4} + \frac{a}{2}\right)$	$f(t) = -A$
	$\left(\frac{3T}{4} + \frac{a}{2}\right)$	to	T	$f(t) = 0$

The function $f(t) = 0$ during three intervals as noted, requiring that the integral be solved for the remaining two intervals.

$$b_n = \frac{2}{T}\int_{\frac{T}{4}-\frac{a}{2}}^{\frac{T}{4}+\frac{a}{2}} A(\sin nwt)dt + \frac{2}{T}\int_{\frac{3T}{4}-\frac{a}{2}}^{\frac{3T}{4}+\frac{a}{2}} -A(\sin nwt)dt$$

$$= \frac{2A}{nwT}\left[(-\cos nwt)_{\frac{T}{4}-\frac{a}{2}}^{\frac{T}{4}+\frac{a}{2}} + (\cos nwt)_{\frac{3T}{4}-\frac{a}{2}}^{\frac{3T}{4}+\frac{a}{2}}\right]$$

$$= \frac{A}{\pi n}\left[(-\cos nwt)_{\frac{T}{4}-\frac{a}{2}}^{\frac{T}{4}+\frac{a}{2}} + (\cos nwt)_{\frac{3T}{4}-\frac{a}{2}}^{\frac{3T}{4}+\frac{a}{2}}\right]$$

To simplify, the following relationships were noted:

$$-\cos nwt\Big]_{\frac{T}{4}-\frac{a}{2}}^{\frac{T}{4}+\frac{a}{2}} = \cos nwt\Big]_{\frac{3T}{4}-\frac{a}{2}}^{\frac{3T}{4}+\frac{a}{2}} : \text{for odd values of n}$$

$$: = 0 \text{ for even values of n}$$

Therefore n will assume only odd values.

$$b_n = \frac{A}{\pi n}\left[-2\cos nwt\right]_{\frac{T}{4}-\frac{a}{2}}^{\frac{T}{4}+\frac{a}{2}}$$

$$= \frac{-2A}{\pi n}\left[\cos\frac{2\pi n}{T}\left(\frac{T}{4}+\frac{a}{2}\right) - \cos\frac{2\pi n}{T}\left(\frac{T}{4}-\frac{a}{2}\right)\right]$$

$$= \frac{-2A}{\pi n}\left[\cos \pi n \left(\frac{1}{2}+\frac{a}{T}\right) - \cos \pi n \left(\frac{1}{2}-\frac{a}{T}\right)\right]$$

A new term was then defined as $S = 2a/T$ (fraction of a square wave with limits. $0 \leq S \leq 1$). Therefore:

$$b_n = \frac{-2A}{\pi n}\cos \pi n \left(\frac{1}{2}+\frac{S}{2}\right) - \cos \pi n \left(\frac{1}{2}-\frac{S}{2}\right)$$

for all odd values of n (1, -1, 3, -3, 5, $\cdots$)

It was noted that a substitution can be made:

$$\cos \pi n\left(\frac{1}{2}+\frac{S}{2}\right) - \cos \pi n\left(\frac{1}{2}-\frac{S}{2}\right) = 2\sin\frac{\pi nS}{2}(-1)^{\frac{n+1}{2}}$$

The expression for b_n was then reduced to:

$$b_n = \frac{-2A}{\pi n}\left[2\sin\frac{\pi nS}{2}(-1)^{\frac{n+1}{2}}\right]$$

$$= (-1)^{\frac{n+3}{2}}\frac{4A}{\pi n}\sin\frac{\pi nS}{2}$$

Leaving the final expression for the Fourier series as

$$f(t) = \sum_{n=1,3,5\cdots}^{n=\infty}(-1)^{\frac{n+3}{2}}\frac{4A}{\pi n}\left(\sin\frac{\pi nS}{2}\right)(\sin nwt)$$

Using the above expression for f(t) a plot of the amplitudes of each harmonic component as a function of the pulse width (δ), which has been defined as fraction of a full square wave, was constructed. This information is presented as Fig. 10. Note that only odd harmonics are present, with peak amplitudes decreasing as the order of the harmonic (n) increases. For a full square wave ($\delta = 1$) the expression is reduced to

$$f(t) = \sum_{n=1,3,5,\cdots}^{n=\infty} (-1)^{\frac{n+3}{2}} \frac{4A}{\pi n} \sin n\omega t$$

which is a familiar equation.

To facilitate experimental procedures the harmonic peak amplitude ratio to the pulse amplitude, as shown in Fig. 10, was converted to RMS voltage values as shown in Fig. 11. The voltage values were based on a constant pulse amplitude of 128 volts. This amplitude is that required to give the fundamental of the square wave pulse a 115 RMS voltage level. Fig. 12 was drawn to illustrate the change in fundamental amplitude caused by a linear variation of pulse width.

The effect of the odd harmonics on the two-phase motor was of prime concern in this investigation. Figs. 10 and 11 show the third harmonic voltage in the pulse to be appreciable for all values of δ except between 0.6 and 0.7. The problem was to determine whether this third harmonic voltage would tend to increase or decrease the output torque, and to determine the magnitude of the change.

For pulse width modulation on the control field only, with rated sine wave excitation on the reference field, there is no third harmonic present in the reference winding. Under these conditions the third harmonic on the control field produces no torque (6). This conclusion was checked experimentally by exciting the test motor reference field with a 400 cycle sine wave, and the control field with a 1200 cycle sine wave supplied by a function generator driving through a 200 watt, high-fidelity amplifier. The reference phase voltage was shifted slowly in phase through 360 degrees by means of a phase shifting network. At no time was any noticeable torque produced, nor did the motor turn with no load.

The situation is more complex when both fields are pulse width modulated, since both the fundamental and all harmonics are present in both fields. Also two different conditions must be considered, that for pulse width greater than 0.67 and that for pulse width less that 0.67. This is indicated by Fig. 11, where the third harmonic curve crosses the zero axis. The phase relationships between motor fields are as shown in the following diagrams:

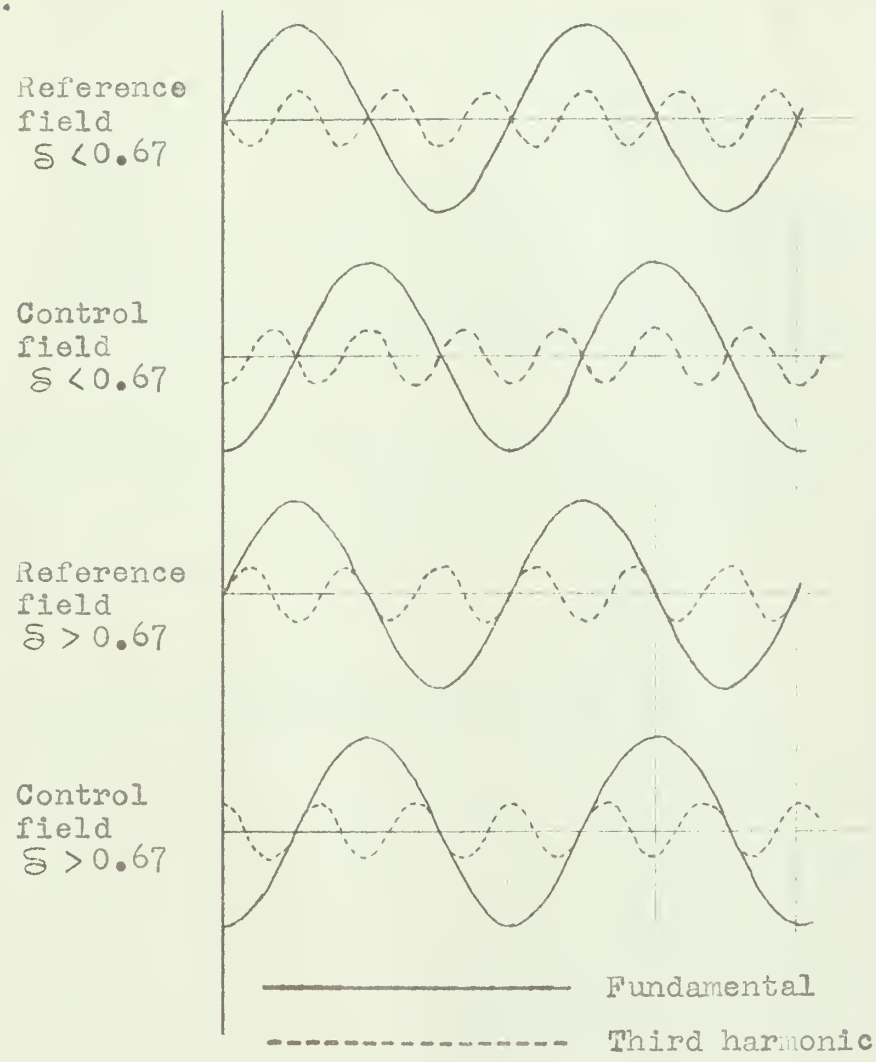

Note that in both cases the reference field fundamental voltage leads the control field fundamental voltage by 90 degrees. Also note that in both cases the third harmonic components are in quadrature, but that the reference field voltage now lags the control field voltage. Thus the torque produced by the third harmonic opposes the fundamental torque for all pulse widths. A similar analysis shows that the fifth harmonic (2000 cycle) produces

a torque which aids the fundamental.

The above conclusions can also be deduced from the Fourier series for the two motor fields:

reference field : $V_r = b_1 \sin \omega t + b_3 \sin 3\omega t + b_5 \sin 5\omega t + \cdots\cdots$

control field : $V_c = b_1 \sin(\omega t - 90^\circ) + b_3 \sin 3(\omega t - 90^\circ) + b_5 \sin 5(\omega t - 90^\circ) + \cdots\cdots$

Note: $\sin 3(\omega t - 90^\circ) = \sin(3\omega t - 270^\circ) = \sin(3\omega t + 90^\circ)$

The statement can now be made that torque produced by higher harmonics will alternately oppose and aid fundamental torque.

3.2 Stall Torque for Various Pulse Widths.

The expected response of the test motor when excited by pulses on both fields was desired. In order to do this it was necessary to calculate the motor response to both 400 cycle and 1200 cycle balanced sine wave excitation. This was first done for stall conditions only (Figs. 3 and 13) and was later extended to produce a complete family of torque-speed curves (Fig. 14).

Stall torque characteristics for balanced sine wave operation were calculated using the equivalent circuit found as shown in Appendix A. The stall torque was computed for various voltage levels for both 400 cycle and 1200 cycle excitation by solving this circuit. Since the input current is an unknown for 1200 cycles, simultaneous equations were required to solve the circuit. A sample

calculation for 30 volts, 400 cycles to each phase follows:

Known initial conditions: (Table I)

V_{in} (per phase) = 30 volts R.M.S, 400 $\sim$

I_{in} (per phase) = 0.28 amperes

P_{in} (per phase) = 14 watts

power factor = $P_{in}/V_{in}I_{in} = 14/(30)(0.28)$

$= 0.625$

power factor angle = $\cos^{-1}(0.625) = 51.3^{\circ}$

Utilizing the motor equivalent circuit as found in Appendix A:

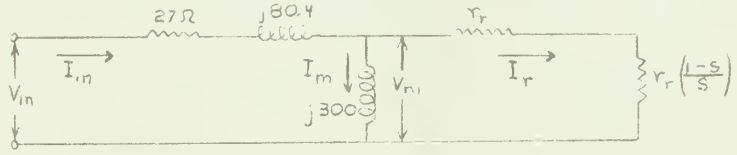

Solving the circuit for I_r in this example:

$V_m = V_{in} - I_{in}Z_s = 26.3 \angle -6^{\circ}$ volts

$I_m = V_m/Z_m = 0.194 \angle -90^{\circ}$ amperes

$I_r = I_{in} - I_m = 0.204 \angle -6^{\circ}$ amperes

(since the phase angle of -6° is small, it was neglected during the remainder of the calculation)

$r_r = V_m/I_r = 286$ ohms

Stall torque may now be determined by the equation:

$$\text{stall torque (in oz)} = \frac{1352}{N_s} P_{rt} \qquad (7)$$

where: N_s = synchronous speed = 12,000 rpm

P_{rt} = total power to rotor = $2I_r^2 r_r$ = 23.6 watts

giving:

$$T_{st} = \frac{1352}{12,000}(23.8) = 2.68 \text{ in oz}$$

This value compares very favorably with the measured stall torque of 2.62 in oz.

The solution of the equivalent circuit for 1200 cycle excitation involved using simultaneous equations, as the input current was not known. Using the same voltage input as for the above sample calculation the stall torque for 1200 cycles was determined as follows:

The equivalent circuit:

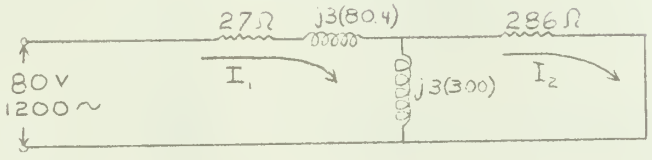

giving the loop equations:

$$80\angle 0 = I_1(27 + j1141.2) - I_2(j900)$$

$$0 = -I_1(j900) + I_2(286 + j900)$$

giving the result: $|I_2| = 0.135$

$$P_{rt} = 2I_2^2 r_r = 2(0.135)^2(286) = 19.6 \text{ watts}$$

$$N_s = 36,000 \text{ rpm}$$

$$T_{st_{1200}} = \frac{1352}{36,000}(19.6) = 0.737 \text{ in oz}$$

The above procedure was repeated for several voltage levels, with the computed values plotted in Fig. 3. This figure shows that computed values are in agreement with the measured values.

A similar solution may be conducted for the fifth

harmonic to show the effect of 2000 cycle signals. The equivalent circuit for this frequency under stall conditions is:

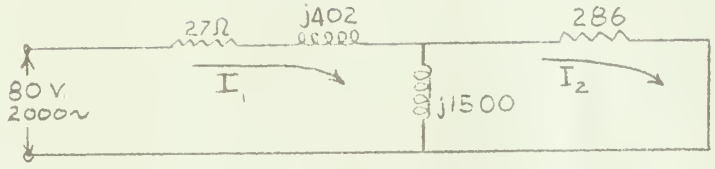

giving the loop equations:

$$80\angle 0 = I_1(27 + j1902) - I_2(j1500)$$

$$0 = -I_1(j1500) + I_2(286 + j1500)$$

giving a result for $|I_2| = 0.148$

$$P_{rt} = 2I_2^2 r_r = 2(0.148)^2 (286) = 12.5 \text{ watts}$$

$$N_s = 60{,}000 \text{ rpm}$$

$$T_{st_{2000}} = \frac{1352}{60{,}000} (12.5) = 0.281 \text{ in oz}$$

This shows the torque of the 2000 cycle component to be about one third of that for 1200 cycles, both figured for an input voltage of 80 volts. Fig. 11 shows that maximum voltage for neither the third nor the fifth harmonic reaches 80 volts. The third harmonic reaches a peak value of 38 volts which would give a maximum stall torque:

$$T_{st_{max}} = \frac{V_{max}}{80} T_{st_{1200}} = \frac{38}{80} (0.737) = 0.35 \text{ in oz}$$

The fifth harmonic attains a peak value of 22.5 volts which would give a maximum stall torque:

$$T_{st_{max}} = \frac{22.5}{80} (0.281) = 0.079 \text{ in oz}$$

This value of torque is quite small compared to the fundamental and third harmonic torques. For this reason the torque due to the fifth and higher harmonics will be considered negligible. This effect was not measured experimentally, but Figs. 14 and 22 indicate that harmonics above the third have negligible effect on the torque.

The finding of stall torque for various pulse widths, with both motor fields pulse width modulated, required an extension of the above procedure. The stall torques for several pulse widths were found be first entering Fig. 11 to obtain the RMS voltage associated with the 400 cycle and 1200 cycle components. Using these voltages the corresponding stall torques were obtained from Fig. 3. Since the 1200 cycle torque opposes the 400 cycle torque the resultant stall torque is the difference between the two component magnitudes.

Example for pulse width (S) = 0.4

$V_{400\sim}$ = 68 volts RMS (Fig. 11)

$V_{1200\sim}$ = -36.2 volts RMS (Fig. 11)

$T_{st_{400}}$ = 1.97 in oz (Fig. 3)

$T_{st_{1200}}$ = -0.12 in oz (Fig. 3)

$T_{st} = |T_{st_{400}}| - |T_{st_{1200}}| = 1.97 - 0.12$

$= 1.85$ in oz

These results were plotted as Fig. 13, showing these computed values in comparison with measured values.

3.3 Computation of Torque-Speed Response.

A rather simple and straightforward procedure was used to compute the expected motor response to pulse width modulation of both motor fields. The current ratio of the third harmonic to the fundamental, determined from Fig. 5, and the voltage ratio of the third harmonic to the fundamental, obtained from Fig. 10 or 11, were used to determine this response. The product of these two ratios gives the current ratio between the 1200 cycle and 400 cycle components of the pulse to be expected for any specific S. Using the current ratio found for a particular S, and the relation that torque is proportional to the current-winding turns product for each winding;

$$T \approx NI$$

the torque due to the third harmonic can be estimated. This was accomplished by multiplying the measured torque for the 400 cycle sine wave excitation from Fig. 2 by the current ratio squared.

A sample calculation for $S = 0.4$:

V_{400} = 67.5 volts RMS (Fig. 11)

V_{1200} = 36.5 volts RMS (Fig. 11)

By interpolating for a winding voltage of 36.5 volts on Fig. 5 the current ratio is obtained:

$$\left.\frac{I_{1200}}{I_{400}}\right]_{36.5V} = \frac{0.090}{0.145} = 0.62$$

the voltage ratio:

$$\frac{V_{1200}}{V_{400}} = \frac{36.5}{67.5} = 0.541$$

giving the overall current ratio:

$$(0.62)(0.541) = \frac{I_{1200}}{I_{400}} = 0.336$$

Since T≈I for each winding the overall torque is proportional to the square of the winding current.

$$T \approx I^2$$

$$\frac{T_{1200}}{T_{400}} = \left(\frac{I_{1200}}{I_{400}}\right)^2 = (0.336)^2 = 0.112$$

This torque ratio signifies the effect of the third harmonic in comparison to the fundamental for a particular pulse width.

The actual values for torque due to the third harmonic were obtained by using this ratio and the value of torque obtained from sine wave excitation as interpolated from Fig. 2 and given directly in Fig. 22. For each speed considered, the torque for a specific voltage, corresponding to the fundamental of a particular pulse width, was picked off. This value was then multiplied by the torque ratio determined for the S concerned, to give the torque due to the third harmonic. The output torque is then given as the difference between the fundamental torque and the third harmonic torque.

The values of torque obtained for various speeds at S = 0.4 are tabulated below along with the measured torques under these conditions for comparison:

Speed rpm	T_{400} in oz	$T_{1200} = T_{400} \times 0.112$	$T_{pulse} = T_{400} - T_{1200}$	T_{pulse} experimental
0	2.60	0.29	2.31	2.30
2000	2.23	0.25	1.98	2.00
4000	1.90	0.21	1.69	1.70
6000	1.54	0.17	1.37	1.35
8000	1.08	0.12	0.96	0.93
10000	0.50	0.06	0.44	0.40

The computed torque-speed response is shown as Fig. 14, with corresponding torque-speed curves for balanced sine wave excitation. The comparison of these two curves shows the greatest effect of the third harmonic to be at narrow pulse widths. This procedure for developing the expected response to a pulse modulated motor appears to be effective, as was later determined by comparison with the measured response.

CHAPTER IV

EXPERIMENTAL EQUIPMENT AND PROCEDURE

4.1 Operation of Pulse Former.

Prior to testing the effects of pulse width modulation on the test motor, it was necessary to develop experimental equipment to produce the necessary fixed and control field voltages to drive the motor. The requirements set for the equipment were that it supply two outputs:

(1) Each to be identical except for a 90 degree phase difference.

(2) Each output to be a constant amplitude, balanced, full wave pulse train, with pulse width continuously variable from a spike to a square wave, having a pulse repetition rate of 400 cycles per second.

(3) One, or both, outputs to have its fundamental (400 cycle) component in quadrature with a 400 cycle, 115 volt source.

The above conditions were met with the equipment shown physically in Fig. 15 and schematically in Fig. 16.

The heart of the pulse forming network is a pair of Reeves Type R-151 resolvers. The rotor shafts of these two resolvers are geared together so that they may be rotated through equal angles, but in opposite directions, by a central shaft. It is characteristic of a resolver that if its two stator phases are excited with equal amplitude

voltages in quadrature with each other (E_1 and $E_1 \angle 90^\circ$), and its rotor is rotated through an angle (θ), the outputs from the rotor will be of equal amplitude and still in quadrature, but displaced by the angle of rotation of the rotor (θ). Thus the outputs of the two resolvers in Fig. 16 are $E_1 \angle \theta$, $E_1 \angle 90^\circ + \theta$, $E_1 \angle -\theta$, and $E_1 \angle 90^\circ - \theta$.

These four outputs from the resolvers are next sent through separate amplifying and clipping circuits to be formed into square waves. By summing these four square waves in alternate pairs two variable width trains of pulses result, in quadrature with each other. The output amplitude is approximately 100 volts, peak to peak. Fig. 17 is a series of scope photographs of the output of one pulse forming network, compared to a 400 cycle voltage. The other pulse train is identical except for being in phase with the 400 cycle sinusoid shown, and thus in quadrature with the pulse train shown.

The sequence of events in the formation of the pulse trains are shown graphically as follows:

Voltage Inputs to Resolvers

E_1

$E_1 \angle 90^\circ$

Resolver Output Voltage ($\theta = 45^\circ$)

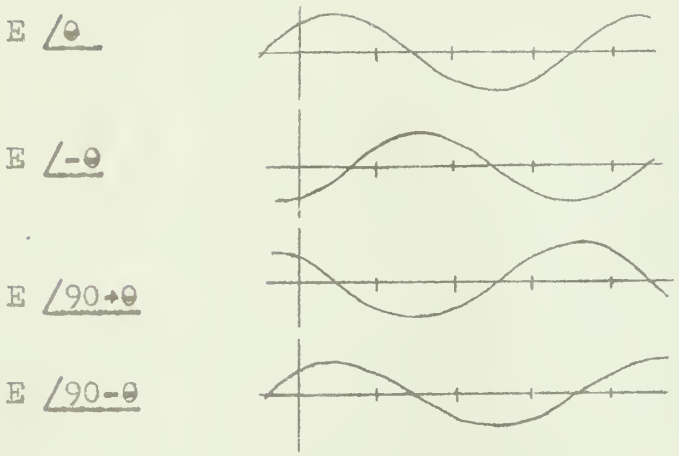

After Clipping

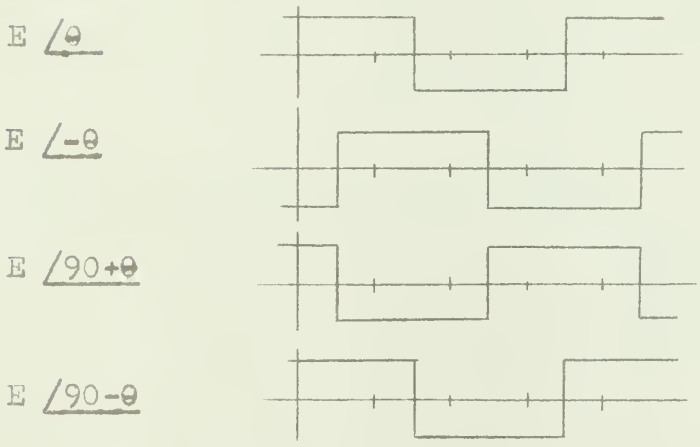

After Summing Pairs

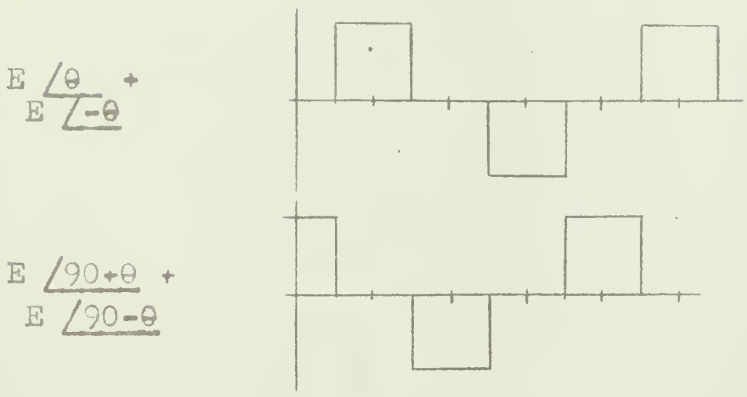

The example shown graphically is for $\theta = 45$ degrees, producing a pulse width of $S = 0.5$. A square wave results if $\theta = 0$ degrees, and complete cancellation occurs when $\theta = 90$ degrees. If θ were increased past 90 degrees, the pulse width would again increase, reaching a full square wave when $\theta = 180$ degrees, but the series would be shifted 180 degrees in phase from that produced when θ was less than 90 degrees. Another 180 degree shift occurs when $\theta = 270$ degrees. This effect is useful if it is desired to vary pulse width in a periodic manner, as for a frequency response, because a complete cycle is accomplished each time the resolvers are turned through 360 degrees.

4.2 Tests Conducted Using the Pulse Former.

Using the pulse forming network to provide driving signals to one or both motor fields, tests were run which paralleled those conducted with standard sinusoidal 400 cycle excitation. Specifically, the following tests were conducted:

a. Torque-Speed, unbalanced; For this test one-half of the pulse former was used to drive the motor control field, while a fixed 115 volt, 400 cycle voltage, in quadrature with the pulse train on the control field (see Fig. 17), was connected to the motor reference field. The experimental setup is shown schematically in Fig. 18. In order to provide sufficient power to drive the motor control phase the pulse former output was connected into a

McIntosh 200 watt power amplifie . In this way a good approximation of rectangular pulses was obtained at the motor terminals. Fig. 19, a and c, are scope photographs of the voltage waveform across the motor control field terminals. Note that the pulse amplitudes are 128 volts, from midpoint to peak, which is the amplitude required to provide a fundamental component of 115 volts RMS for a square wave. Parts b and d of Fig. 19 are scope photographs of the voltage across a one ohm pure resistance (a length of straight nichrome wire) in series with the control field. It was necessary to place a decade capacitor across the McIntosh amplifier output in order to balance the load to the amplifier. A capacitance of 0.5 microfarads was the average value used. Pulse width and pulse amplitude measurements were made on a Tektronix Type 515 oscilloscope. The same scope was used for all experimental measurements to provide a constant measurement standard. The torque-speed curves obtained by the above procedure are plotted on Fig. 20 (dashed curves). The sine wave, amplitude modulated curves (solid curves) shown for comparison on Fig. 20 were obtained using the same Tektronix oscilloscope for voltage measurements. The uppermost dashed curve ($S = 0.7$) is not considered to be a true indication of performance because it was not possible to obtain a pulse amplitude of 128 volts near stall at this pulse width without considerable distortion, due to amplifier limitations.

b. Torque-Speed, balanced: Details of this test are the same as for the unbalanced torque-speed tests, except that both outputs of the pulse former were used, driving both motor fields through McIntosh amplifiers. Fig. 18-b is a schematic of the experimental setup, while Fig. 21 is a photograph of the same setup. Once again the Tektronix oscilloscope was used for all voltage and pulse width measurements, a switch being provided to permit alternate viewing of the two pulse trains. A series of runs were also made for balanced 400 cycle sine wave excitation, using the oscilloscope for voltage measurements, to provide directly comparable curves. These two sets of curves are plotted as Fig. 22.

c. Frequency Response: The motor response to a variable frequency, pulse width modulated signal, was studied by means of the experimental setup shown schematically in Fig. 23, and physically in Fig. 24. A two-phase motor was used to drive the resolvers of the pulse forming network at variable speed, thereby producing pulses with widths varying linearly with time. Each revolution of the drive motor caused pulse width to vary through a complete cycle, that is from a null to a square wave, back to a null, then through the same variation but shifted 180 degrees in phase. Fig. 12 illustrates this variation of pulse width, and also the variation of fundamental (400 cycle) amplitude, with time. It is to be noted that although pulse width varies

linearly with time, the amplitude of the fundamental varies sinusoidally with time. Referring again to Fig. 23, it is seen that a 400 cycle tachometer was used as a transducer, and an oscilloscope as the measuring device. The scope was synchronized with the pulse input to the motor control phase, and a switch permitted alternate viewing of motor input and tachometer output waveforms. In this way it was possible to obtain comparitive amplitude and phase shift information from the oscilloscope. Frequency was also measured on the oscilloscope, and checked with a stop watch and counter. The velocity response information obtained by the above method is displayed on Fig. 25 for two different pulse amplitude levels. The frequency response obtained from the 40 volt velocity response is plotted on Fig. 26, along with the previously determined frequency response for 400 cycle sinusoidal excitation for comparison purposes.

d. Stall Temperature Measurements: In order to provide comparative temperature figures for standard and pulsed excitation, a series of stall temperature runs were conducted. For these tests the motor was preheated to a temperature of 70 degrees Centigrade, the voltage levels set at the desired values, and the motor stalled for ten minutes. Temperature readings were taken at one minute intervals to note the trend of heating, and a final temperature reading taken at the end of the ten minute stalled

period. A thermocouple set in a hole drilled in the motor case was used in conjunction with a thermocouple bridge to measure temperature. The case temperatures recorded after ten minutes at stall are plotted on Fig. 27. Each curve is for a different type of excitation, and separate points on the curves are for different amplitudes of excitation. From these curves it is apparent that a slightly greater heating effect is associated with pulsed excitation than with sine wave excitation.

CHAPTER V

RESULTS OF INVESTIGATION

5.1 Results and Discussion:

From the information presented thus far in this investigation, the feasibility of driving a two-phase servomotor with pulses can be determined. All information collected is for one specific motor, but in general would be valid for any small two-phase servomotor.

This study has shown that for unbalanced conditions, with only the control field pulse width modulated, the third harmonic (and higher harmonics) has no effect on the motor's torque-speed response (Fig. 20) or frequency response (Fig. 26). This result is readily apparent, as there is no 1200 cycle component in the reference field to develope a rotating field.

Operating the motor under balanced pulsed conditions introduces the effect of harmonics (Figs. 14 and 22). Only the third harmonic has a noticeable effect, this being greatest at narrow pulse widths and becoming insignificant at pulse widths larger than $\delta = 0.5$. At a pulse width of $\delta = 0.2$ the computed torque output is down 33 per cent from torque of normal sine wave motor operation, as shown in Fig. 14. The experimental results for these same conditions show the torque under pulsing to be down only 25 per cent (Fig. 22), so the computed effect is pessimistic.

In some control motor applications this loss of torque would be unacceptable, where maximum torque is needed for small errors. For a majority of applications this loss of torque would be of little significance compared to the gains possible by using this system.

The temperature runs, as shown by Fig. 27, indicate that the pulsed motor had a slightly higher temperature, after being stalled for ten minutes, than did the motor under normal excitation. For narrow pulse widths the temperature difference reached a maximum of seven degrees Centigrade for balanced conditions, and four degrees Centigrade for unbalanced conditions. Fig. 27 also shows the temperature to be lower for motor operation under balanced conditions than under unbalanced conditions. This condition is a result of the continuous large I^2R loss in the reference field of the unbalanced operated motor. Thus for maximum savings in heat generation the motor could be operated under balanced conditions. For many applications this would not be practical, when maximum torque at small errors is a necessity. For a control system which spends a large protion of the time at rest, or a positioning system where the error signal is zero a major part of the time, the heat saved by eliminating the constant current flow in the reference field of the motor might be worthwhile.

It must be remembered that these temperature measurements were taken after the motor had been stalled for ten

minutes, a condition which is far more severe than would be encountered in practice. For average motor operation it is considered that the temperatures produced by pulsing would be negligibly different from those produced by normal excitation.

It is considered that the operation of a two-phase servomotor under pulsed excitation is feasible and practical for most applications. The development of a power amplifier using switching transistors should be continued, in order to build up a system which operates more efficiently and with less heat dissapation than present amplitude modulated systems using linear power amplifiers. This development was discussed in more detail in Chapter I.

Another possibility for the use of pulse width modulation of a servomotor is in conjunction with information telemetering. The use of the pulse width modulated error signal of the servo system as a measurement of a desired quantity to trigger the transmitter of a pulse width modulated telemetering system would save on equipment and weight. This consideration features some favorable possibilities which is suggested for further investigation.

The integration of the pulse width modulated two-phase servomotor in a closed loop servo system is left for further development and study.

5.2 Conclusions:

This investigation was concerned primarily with the effects of various width pulse signals on the torque-speed response of a typical small two-phase servomotor. Other effects of interest were those of heating and the frequency response. This study predicted the effects mathematically and measured them experimentally for both balanced and unbalanced operation of the motor. The conclusions of this investigation may be summarized as follows:

1) Pulse width modulation of the control field only with normal 400 cycle sinusoidal voltage on the reference field (unbalanced operation) has no effect from the third or higher harmonics. The effect is the same as for amplitude modulation of the control field.

2) Pulse width modulation of both fields (balanced condition) showed no effects of harmonics higher than the third harmonic.

3) The torque produced by the third harmonic opposed the torque produced by the fundamental. This decreased the total motor output torque. The effect of the third harmonic was greatest for narrow pulse widths where the voltage ratio of the third harmonic to the fundamental was greatest.

4) Heating effects of the pulse width modulation were a slight increase in temperature over the temperatures of normal operation. This increase in temperature may be

considered negligible. For narrow pulses the heat generated is less when the motor is operating under balanced conditions.

5) It is feasible and practical to operate a servomotor with pulse width modulated signals.

APPENDIX A

DETERMINATION OF AN EQUIVALENT CIRCUIT

An equivalent circuit was determined for balanced operating conditions of the motor, using values recorded during the torque-speed measurements and listed in Table I. Using the approximate equivalent circuit for a two-phase servomotor as given in references 9 and 10:

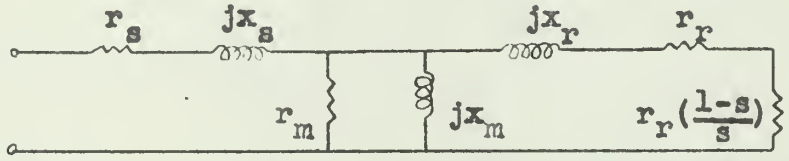

where r_s = stator winding resistance of one phase, both phases considered to be identical.

x_s = reactive impedance of stator winding.

r_m = core loss and iron loss resistance of winding.

x_m = air gap inductance.

x_r = rotor reactive impedance reflected into stator winding.

r_r = rotor resistance reflected into stator winding.

s = slip = $\frac{\text{synchronous speed - rotor speed}}{\text{synchronous speed}}$

The value of r_s used was 27 ohms, a mean value, as the variation with operating temperature was from 24.5 ohms to 29.5 ohms. This resistance was measured with an impedance bridge. The inductance of the stator winding was also measured with an impedance bridge, with the rotor removed

and the other stator winding short circuited, giving a value of 0.032 henries. Therefore:

$$x_s = 2\pi(400)(0.032) = 80.4 \text{ ohms}$$

To determine Z_m (parallel combination of r_m and x_m) the motor was considered to be under no load balanced conditions for several voltages. Under these conditions the rotor current could be considered negligible. The input impedance, Z_{in}, was determined from voltage, current, and power values from Table I. The equations used, along with a corresponding set of sample values, follow:

$$Z_{in} = r_s + jx_s + Z_m = R + jX = 383\underline{/78.6^\circ} \text{ ohms}$$

$$R = Z_{in}\cos(78.6) = 75.5 \text{ ohms}$$

$$X = Z_{in}\sin(78.6) = 375 \text{ ohms}$$

$$Z_m = (R - r_s) + j(X - x_s) = \frac{r_m(jx_m)}{r_m + jx_m}$$

$$R - r_s = \frac{r_m x_m^2}{r_m^2 + x_m^2} = x_m \frac{r_m x_m}{r_m^2 + x_m^2} = 48.5 \text{ ohms}$$

$$j(X - x_s) = \frac{jr_m^2 x_m}{r_m^2 + x_m^2} = r_m \frac{jr_m x_m}{r_m^2 + x_m^2} = j294.6 \text{ ohms}$$

Since computed values of r_m and x_m varied over a narrow range for different experimental runs, mean values were determined:

$$r_m \text{ (average)} = 1845 \text{ ohms}$$

$$x_m \text{ (average)} = 300 \text{ ohms}$$

In this parallel combination r_m is greater than x_m by a factor of six or greater, so the value of r_m may safely be neglected, and the effective value of Z_m is:

$$Z_m \text{ (average)} = jx_m \text{ (average)} = j300 \text{ ohms}$$

The determination of Z_r (x_r, r_r, and $r_r\frac{1-s}{s}$) required using measured values of current and voltage input for each load condition. By means of circuit reduction, using Ohm's law and Kirchoff's laws, values of Z_r were found as follows:

$$I_s = I_r + I_m = 0.320\angle -67.5 \text{ amperes}$$

$$V_m = V_{in} - I_s Z_s = 115\angle 0 - (0.320\angle -67.5)(84.8\angle 71.4)$$

$$= 87.8\angle -2.0 \text{ volts}$$

$$I_m = V_m/Z_m = \frac{87.8\angle -2}{300\angle 90} = 0.292\angle -92 \text{ amperes}$$

$$I_r = I_s - I_m = 0.320\angle -67.5 - 0.292\angle -92$$

$$= 0.122\angle -6.0 \text{ amperes}$$

$$Z_m = \frac{E_m}{I_r} = \frac{87.8\angle -2.0}{0.122\angle -6.0} = 718\angle 4.0 \text{ ohms}$$

The angle associated with Z_r was found to be always smaller than five degrees, therefore in further calculations the reactive component was neglected and Z_r considered to be a pure resistance:

$$Z_r = r_r + r_r\frac{1-s}{s} = \frac{r_r}{s} = 718 \text{ ohms}$$

$$s = \frac{12{,}000 - 9050}{12{,}000} = 0.246$$

$$r_r = sZ_r = (0.246)(718) = 176 \text{ ohms}$$

The values of r_r found by the above method were found to be different for each voltage level and rotor speed, varying as shown in Fig. 6. This variation indicates that a single equivalent circuit is a good approximation of the motor only for a limited speed and voltage range.

The values of r_r determined were checked by computing the power out, using the equation for one winding and doubling the result:

$$P_{out} = 2\, I_r^2 r_r \left(\frac{1-s}{s}\right) = 2(0.0149)(176)\left(\frac{0.754}{0.246}\right)$$
$$= 14.6 \text{ watts} \qquad (7)$$

This value of power was checked with power determined from torque and speed measurements in Table I. This experimental value of P_{in} was 13.0 watts, which is in good agreement with the calculated value from the equivalent circuit.

The final equivalent circuit obtained by this development, and to be used during this investigation, is:

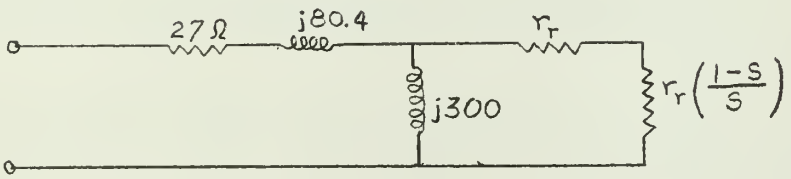

with values of r_r to be taken from Fig. 6.

BIBLIOGRAPHY

1. Milnes, A.G.; Transistor Power Amplifier with Switched Mode of Operation, AIEE Transactions, Vol. 75, 1956

2. Thaler, G.J.; Elements of Servomechanism Theory, McGraw-Hill Co., New York, 1955

3. Stein, W.A. and Thaler, G.J.; Evaluating the Effect of Non-linearity in a 2-Phase Servomotor, AIEE Transactions, January 1955

4. Ellett, D.M.; How to Determine Mass Moments of Inertia for Irregular Parts, Product Engineering, May 1957

5. Ritow, I.; Using Fourier Analysis in Designing, Electrical Manufacturing, Feb. 1959

6. Busey, C.W. and Bartow, W.R.; The Effect of Non-Sinusoidal Impressed Voltages on A.C. Servomotors, Thesis, USNPS 1955

7. Truxel, J.G.; Control Engineers Handbook, McGraw-Hill Co., New York, 1958, chapter 12

8. Eshbach, O.W.; Handbook of Engineering Fundamentals, 2nd. ed., John Wiley & Sons, Inc., New York, 1952

9. Gibson, J.E. and Tuteur, F.B.; Control System Components, McGraw-Hill Co., New York, 1958

10. Fitzgerald, A.E. and Kingsley, C.; Electric Machinery, 1st. ed., McGraw-Hill Co., New York, 1952

11. Mikhail, S.L. and Fett, G.H.; Transfer Function of 2-Phase Servomotors, AIEE Transactions, Vol. 77, 1958

12. Churchill, R.V.; Fourier Series and Boundary Value Problems, McGraw-Hill Co., New York, 1941

13. Koopman, R.J.W.; Operating Characteristics of Two-Phase Servomotors, AIEE Transactions, Vol. 68, 1949

14. Keegan, A.J.; Transistor Servo Amplifier Output Stages, Semiconductor Products, Vol. 1, June 1958

15. Thaler, G.J. and Brown, R.G.; Servomechanism Analysis, McGraw-Hill Co., 1953

16. Lawrence, R.R. and Richards, H.E.; Principles of Alternating-Current Machinery, 4th. ed., McGraw-Hill Co., 1953

17. Brown, G.S. and Campbell, D.P.; Principles of Servomechanisms; John Wiley & Sons, Inc., New York, 1948

TABLE I

TORQUE-SPEED MEASUREMENTS FOR BALANCED CONDITIONS OF SERVOMOTOR OPERATION

volts	speed rpm	torque in oz	Reference phase I ma	Reference phase P watts	Reference phase power factor	Reference phase Z ohms	Control phase I ma	Control phase P watts	power out watts	Temperature °C case	Temperature °C winding
115	11750	0	300	6.8	.197	383	308	7.1	0	55.0	63.5
	10710	0.84	305	9.4	.268	377	310	10.2	6.74	55.0	63.5
	9050	1.95	320	14.1	.382	359	322	15.0	13.0	55.5	65.0
	8000	2.50	330	16.6	.446	348	332	17.7	14.5	58.0	68.8
	6430	3.30	345	20.0	.505	333	348	21.0	15.8	65.5	77.5
	4970	3.92	365	23.3	.555	315	367	24.2	14.4	74.0	89.0
	3350	4.50	380	25.8	.600	303	386	26.8	11.3	85.0	101.0
	1910	4.92	395	27.6	.606	291	398	28.9	7.0	95.0	110.0
	970	5.15	402	28.6	.627	286	405	30.1	3.74		
	0	5.48	411	30.0	.635	280	411	31.3	0.0		
100	11700	0.0	230	6.7	.220	435	232	6.9	0.0		
	10170	0.80	242	7.2	.297	413	242	7.5	6.31	61	
	8840	1.52	275	11.1	.400	364	274	11.3	9.85	62	
	7400	2.15	288	14.0	.486	347	288	14.3	11.3	68.5	

TABLE I

volts	speed	torque	Reference Phase				Control Phase		power out	Temperature	
			I	P	p.f.	Z	I	P		case	winding
100	5640	2.88	305	17.1	.561	328	304	17.6	12.0		
	3950	3.42	326	19.5	.598	307	329	20.3	10.0		
	2490	3.85	341	21.2	.621	294	343	22.2	7.2		
	1180	4.18	352	22.6	.641	284	357	23.9	3.61		
	0	4.50	365	24.0	.658	274	370	25.2	0.00		
80	11690	0.0	188	3.6	.239	426	184	3.8	0.00		
	9580	0.70	200	5.7	.366	400	190	5.7	5.72	63.0	69.3
	7940	1.15	210	7.2	.448	381	200	7.5	6.80	65.0	71.8
	6550	1.50	222	8.8	.495	360	215	9.1	7.20		
	5340	1.75	232	10.0	.551	345	225	10.3	7.00	68.5	74.8
	4060	2.00	245	10.9	.558	327	238	11.2	6.00		
	2900	2.15	255	11.6	.587	314	248	12.1	4.62		
	1910	2.35	262	12.2	.592	305	257	12.7	3.38		
	1040	2.42	270	12.8	.611	296	264	13.3	2.17		
	0	2.62	280	13.2	.616	286	272	14.0	0.00		

TABLE I

volts	speed	torque	Reference Phase				Control Phase		power out	Temperature	
			I	P	p.f.	Z	I	P		case	winding
60	11610	0.00	119	1.0	.140	504			0.00		
	7960	0.65	145	3.9	.448	414	138	3.9	3.64	70.5	
	7060	0.80	150	4.3	.478	400	140	4.5	4.10	75.0	
	5600	0.95	160	5.2	.542	375	150	5.2	3.96	79.0	
	4360	1.10	170	5.9	.578	353	160	5.9	3.52	81.0	
	3640	1.15	178	6.1	.574	337	168	6.2	3.10	83.0	
	2630	1.30	185	6.6	.595	324	177	6.7	2.55	84.0	
	1190	1.45	202	7.1	.586	298	190	7.2			
	0	1.57	210	7.6	.603	285	200	7.7	0.00		
40	9400	0.00	75	0.9	.300	534					
	4280	0.50	100	2.1	.525	400	100	2.1		73.0	81.5
	3250	0.50	118	2.3	.500	339	112	2.3		71.0	81.3
	1920	0.60	125	2.5	.520	320	114	2.5			
	1160	0.62	130	2.8	.550	308	120	2.7			
	0	0.65	130	3.0	.577	307	125	3.0			

FIGURE 1

TORQUE - SPEED CHARACTERISTICS
OF
AMERICAN ELECTRONICS SERVOMOTOR

FIXED PHASE EXCITATION – 115 V 400 ~
CONTROL PHASE – VARIABLE 400 ~

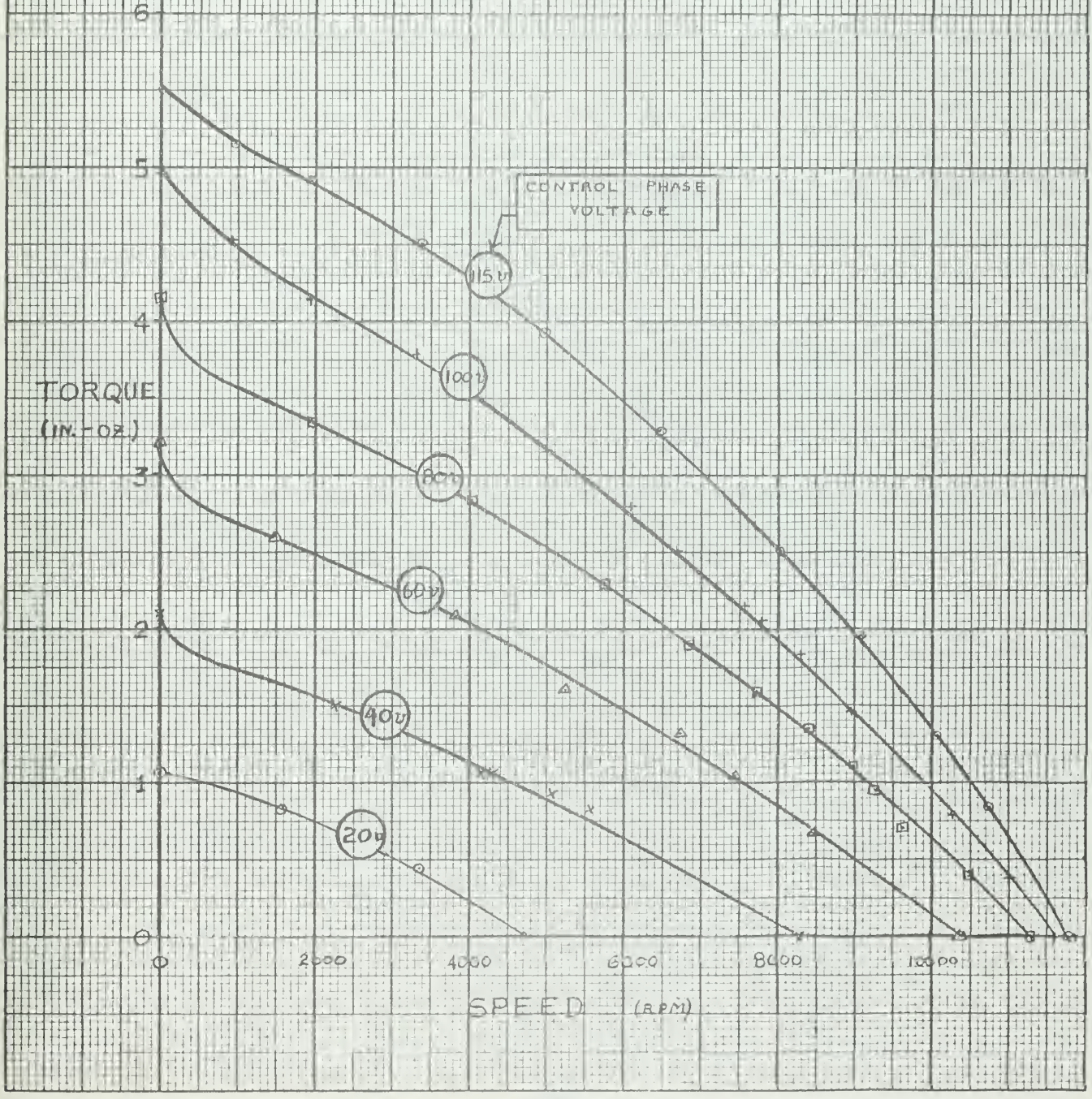

FIGURE 2

TORQUE-SPEED CHARACTERISTICS
OF
AMERICAN ELECTRONICS SERVOMOTOR
BALANCED PHASE EXCITATION - 400 ~

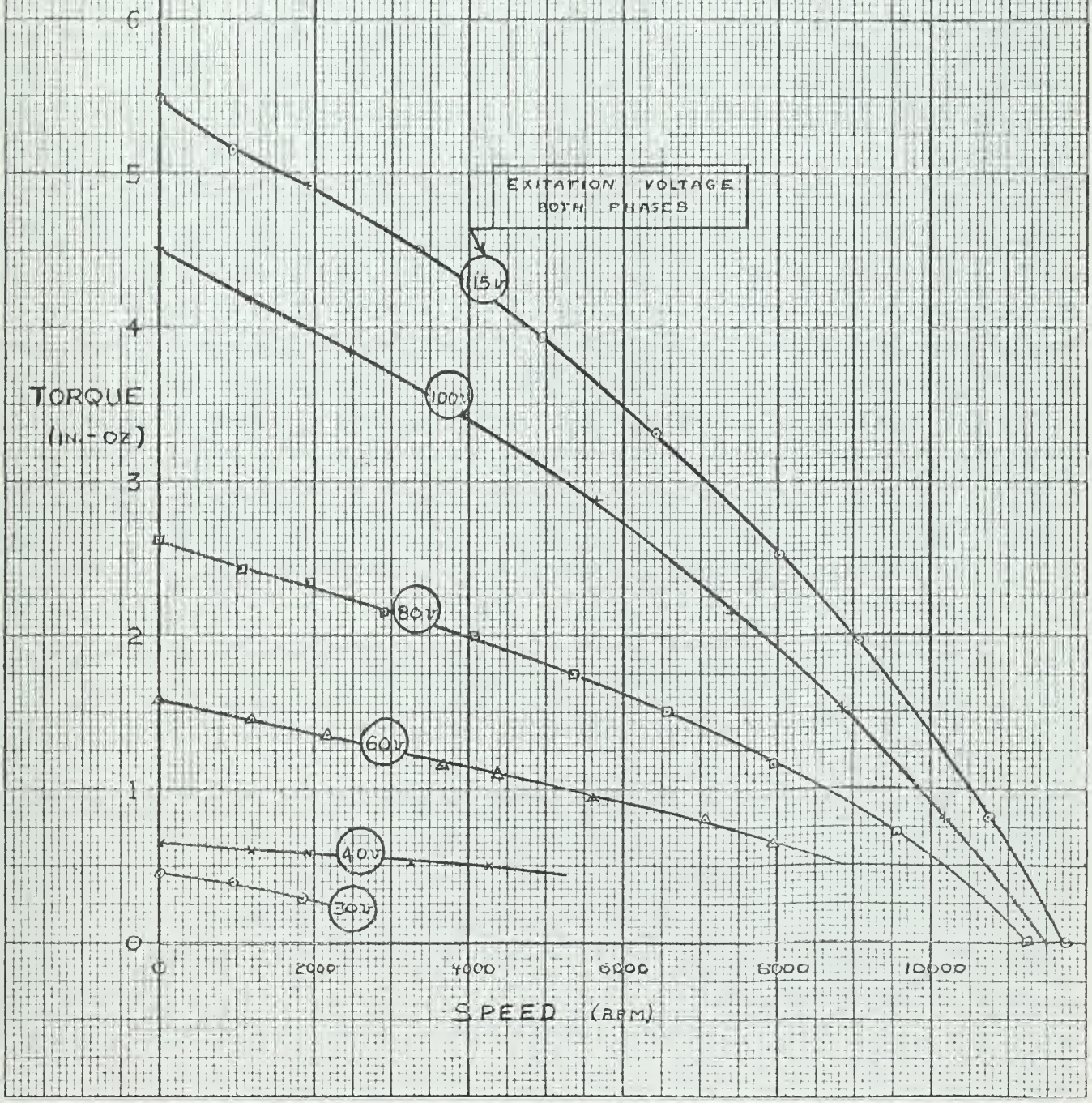

FIGURE 3

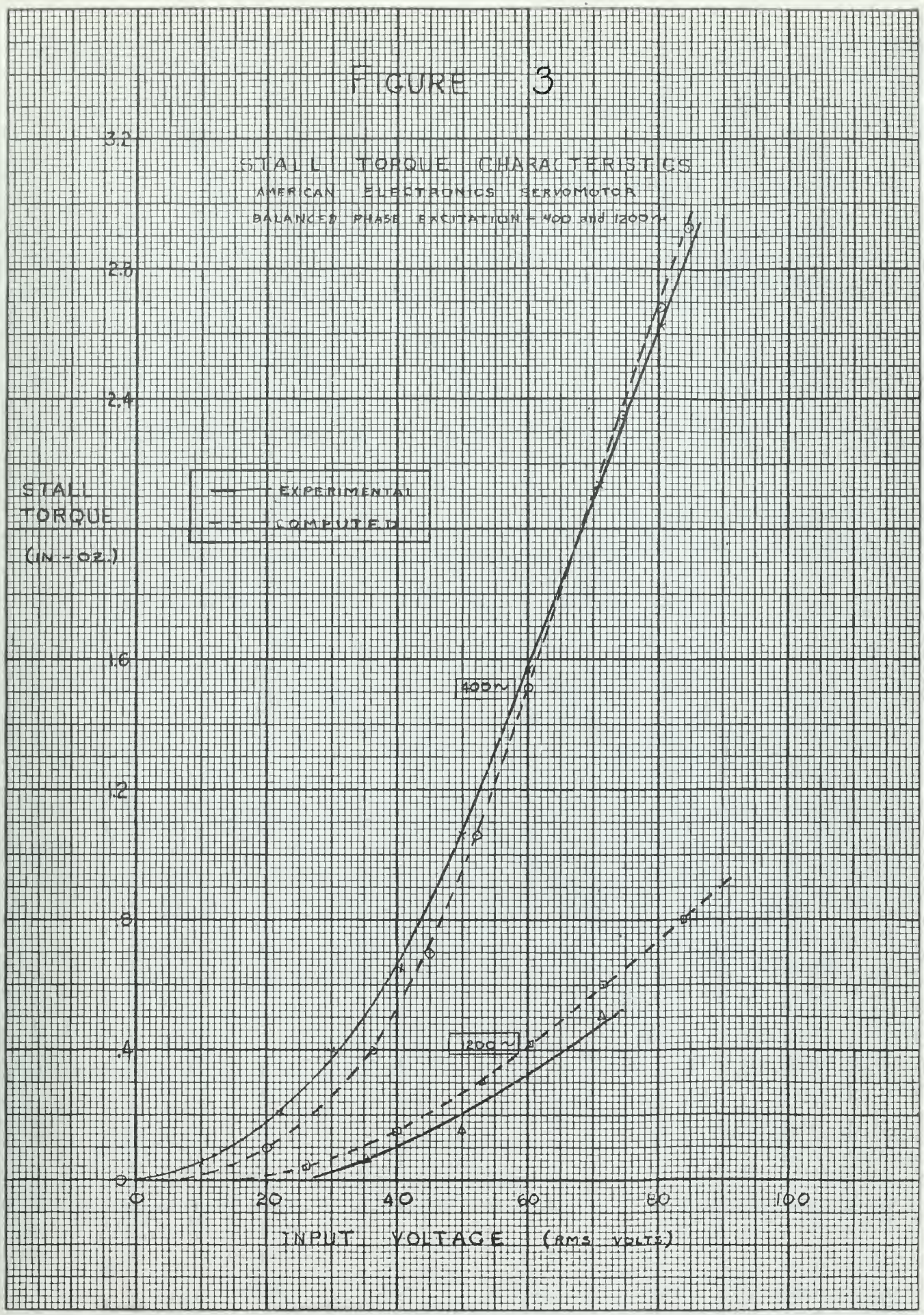
STALL TORQUE CHARACTERISTICS
AMERICAN ELECTRONICS SERVOMOTOR
BALANCED PHASE EXCITATION - 400 and 1200 ~
STALL TORQUE (IN.-OZ.)
EXPERIMENTAL
COMPUTED
400 ~
1200 ~
3.2
2.8
2.4
1.6
1.2
.8
.4
0
0
20
40
60
80
100
INPUT VOLTAGE (RMS VOLTS)

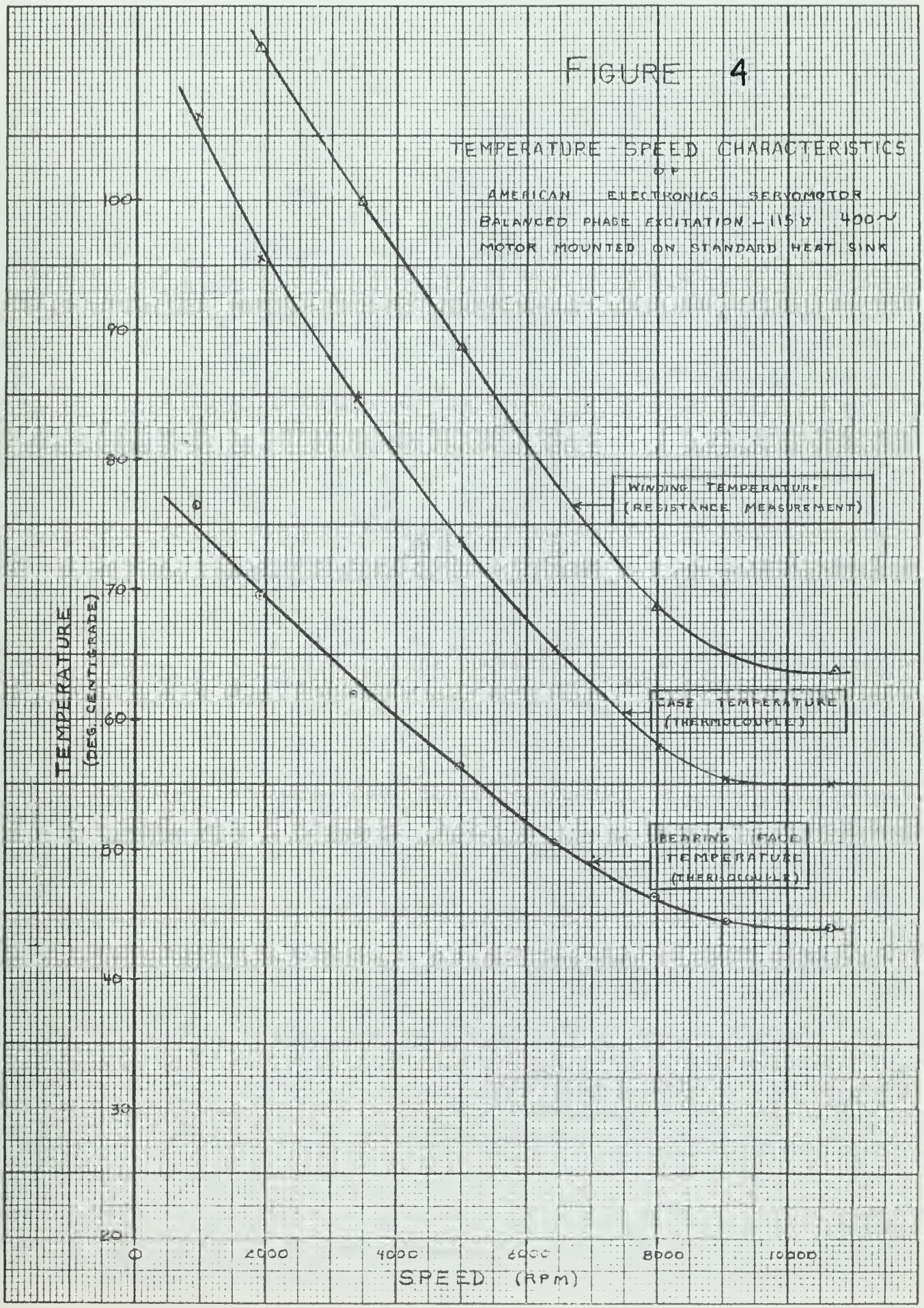
FIGURE 4
TEMPERATURE - SPEED CHARACTERISTICS
OF
AMERICAN ELECTRONICS SERVOMOTOR
BALANCED PHASE EXCITATION — 115 V 400~
MOTOR MOUNTED ON STANDARD HEAT SINK
WINDING TEMPERATURE (RESISTANCE MEASUREMENT)
CASE TEMPERATURE (THERMOCOUPLE)
BEARING FACE TEMPERATURE (THERMOCOUPLE)
TEMPERATURE (DEG. CENTIGRADE)
100
90
80
70
60
50
40
30
20
0
2000
4000
6000
8000
10000
SPEED (RPM)

FIGURE 5

STATIC WINDING CURRENT OVER FREQUENCY RANGE

AMERICAN ELECTRONICS SERVOMOTOR

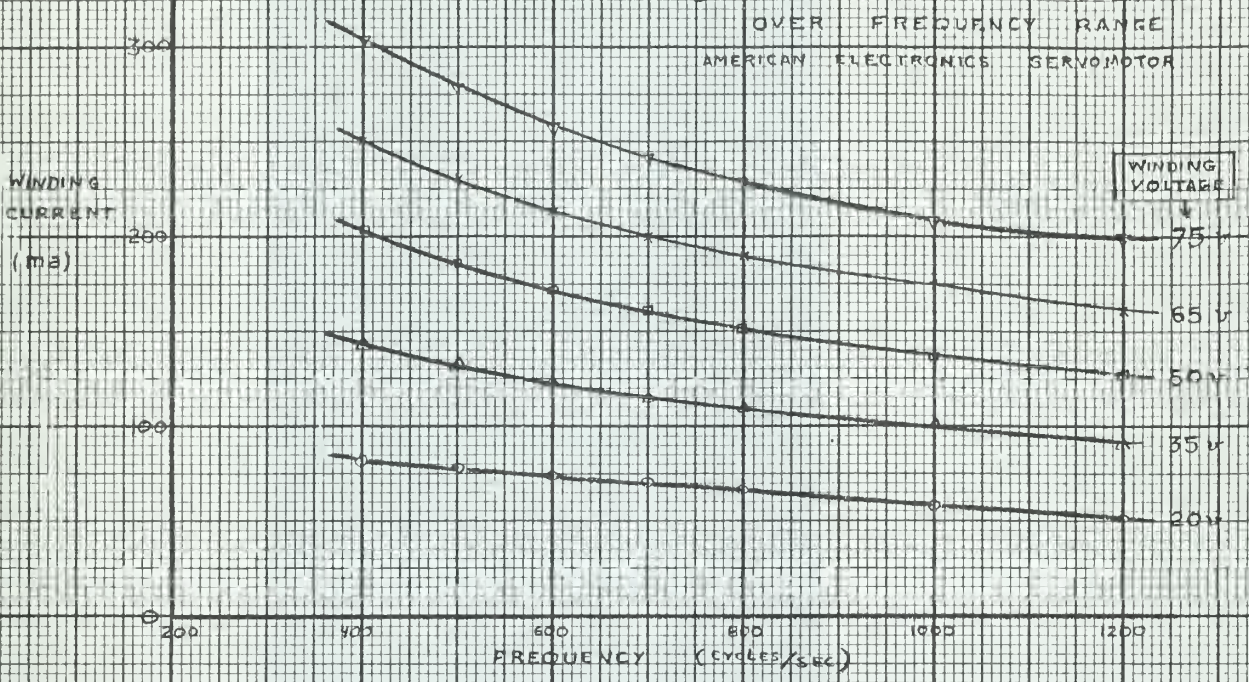

FIGURE 6

REFLECTED ROTOR RESISTANCE

VARIATIONS WITH SLIP AND VOLTAGE

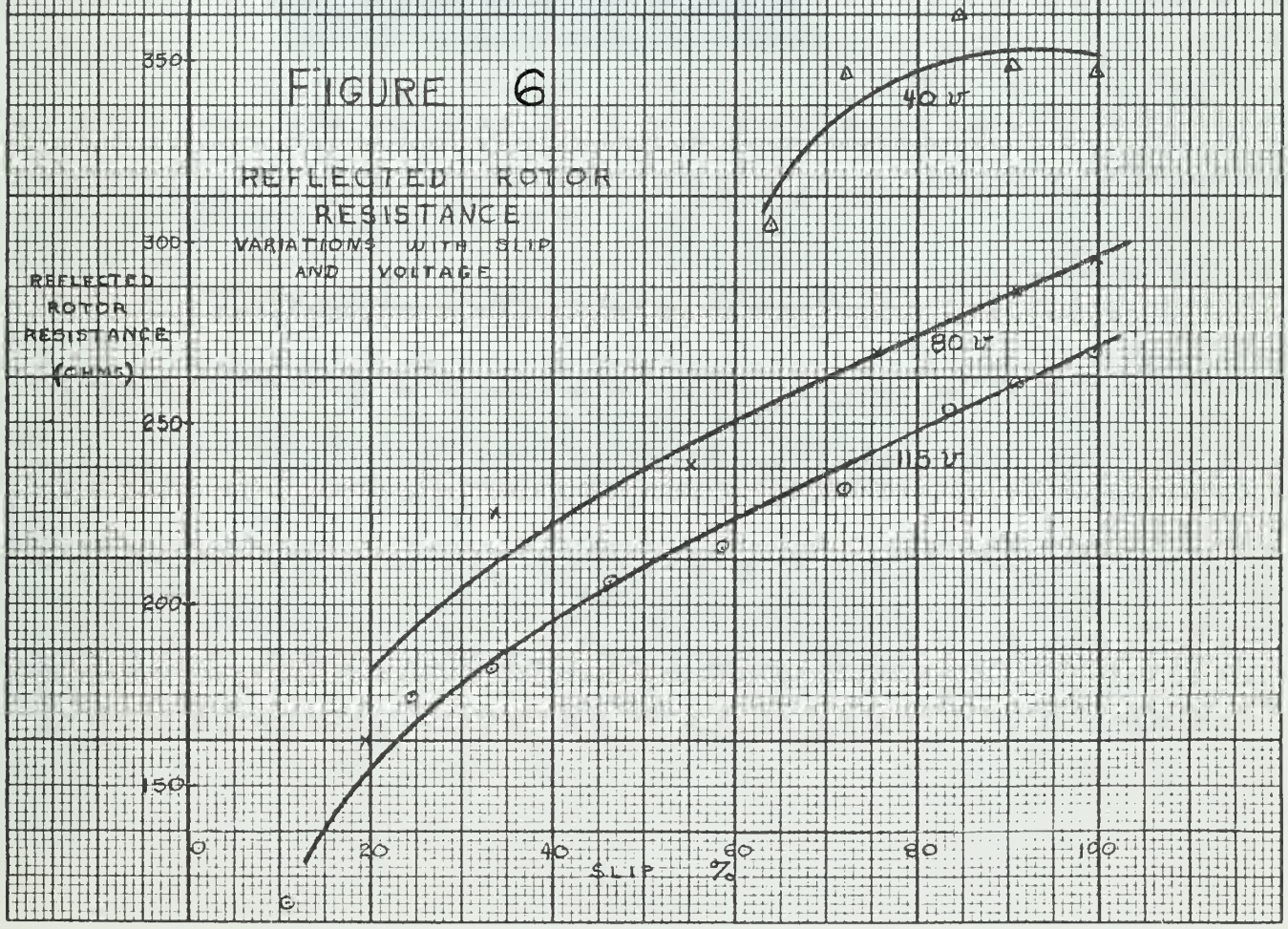

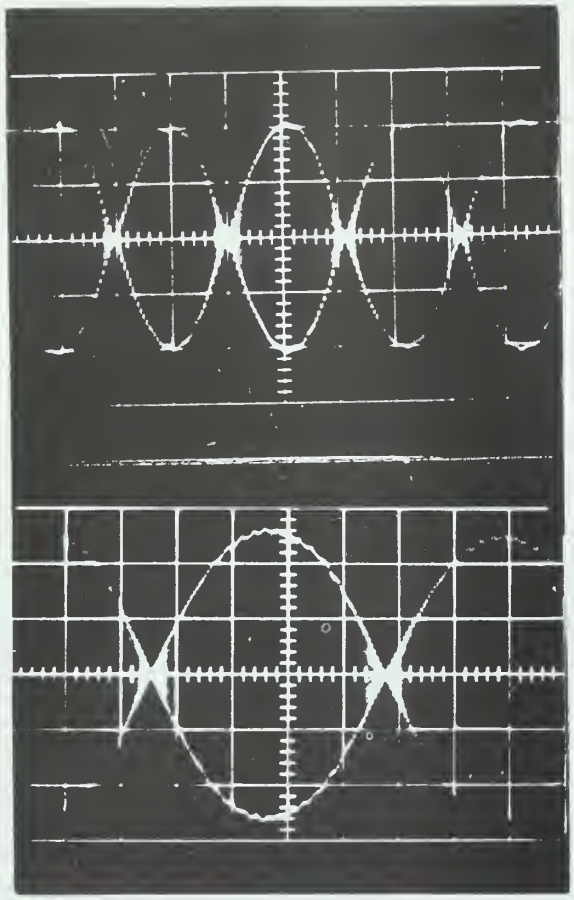

FIGURE 7

Frequency Response Test.

Tachometer Output from

Sinusoidal Modulation of

Servomotor

scale: vert. 50 volts/line
horiz. 50 msec /line

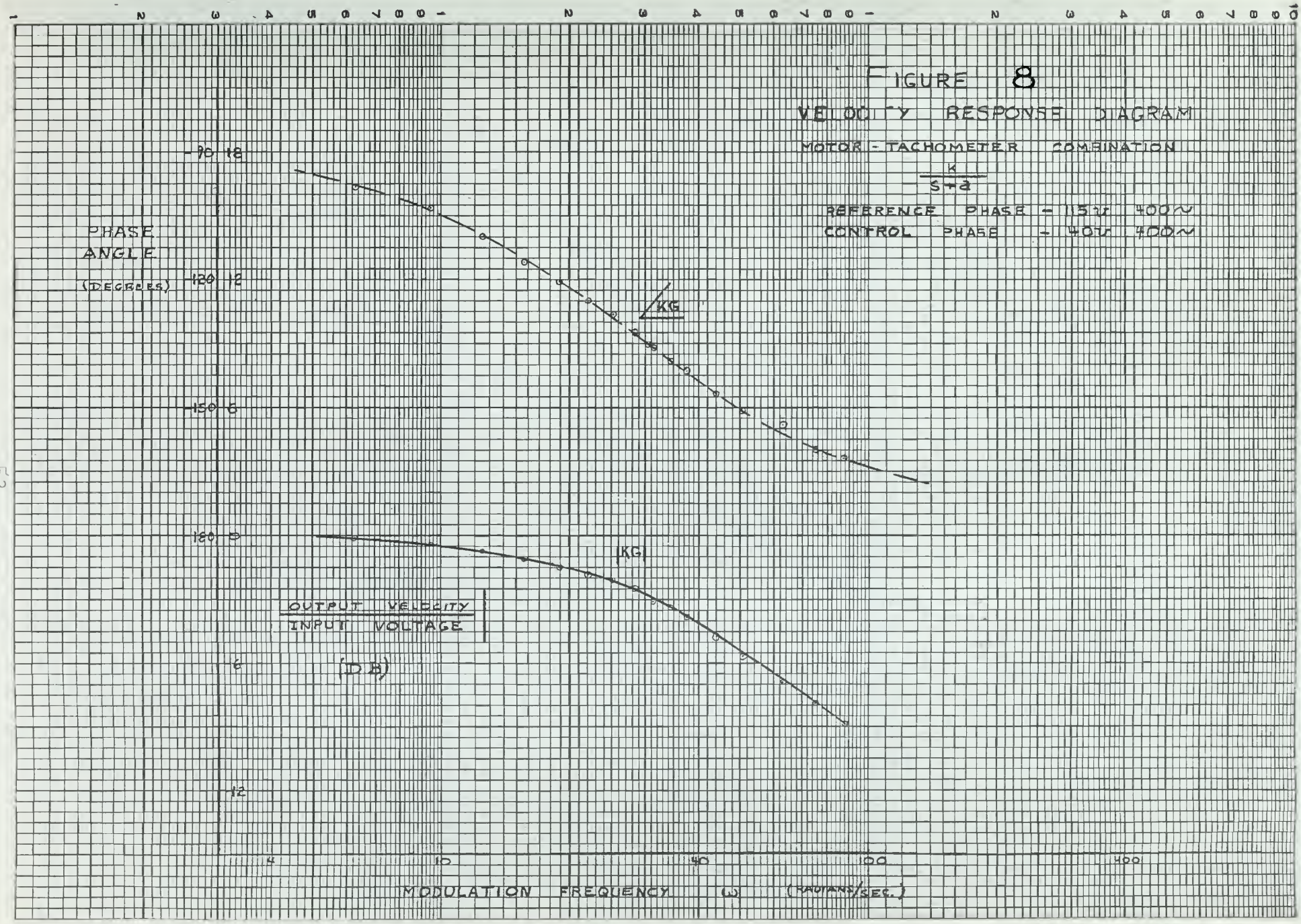
FIGURE 8
VELOCITY RESPONSE DIAGRAM
MOTOR - TACHOMETER COMBINATION
K / S+a
REFERENCE PHASE - 115V 400~
CONTROL PHASE - 40V 400~
PHASE ANGLE (DEGREES)
-90
-120
-150
-180
KG
|KG|
OUTPUT VELOCITY / INPUT VOLTAGE
(DB)
18
12
6
0
-6
-12
4
10
40
100
400
MODULATION FREQUENCY ω (RADIANS/SEC.)

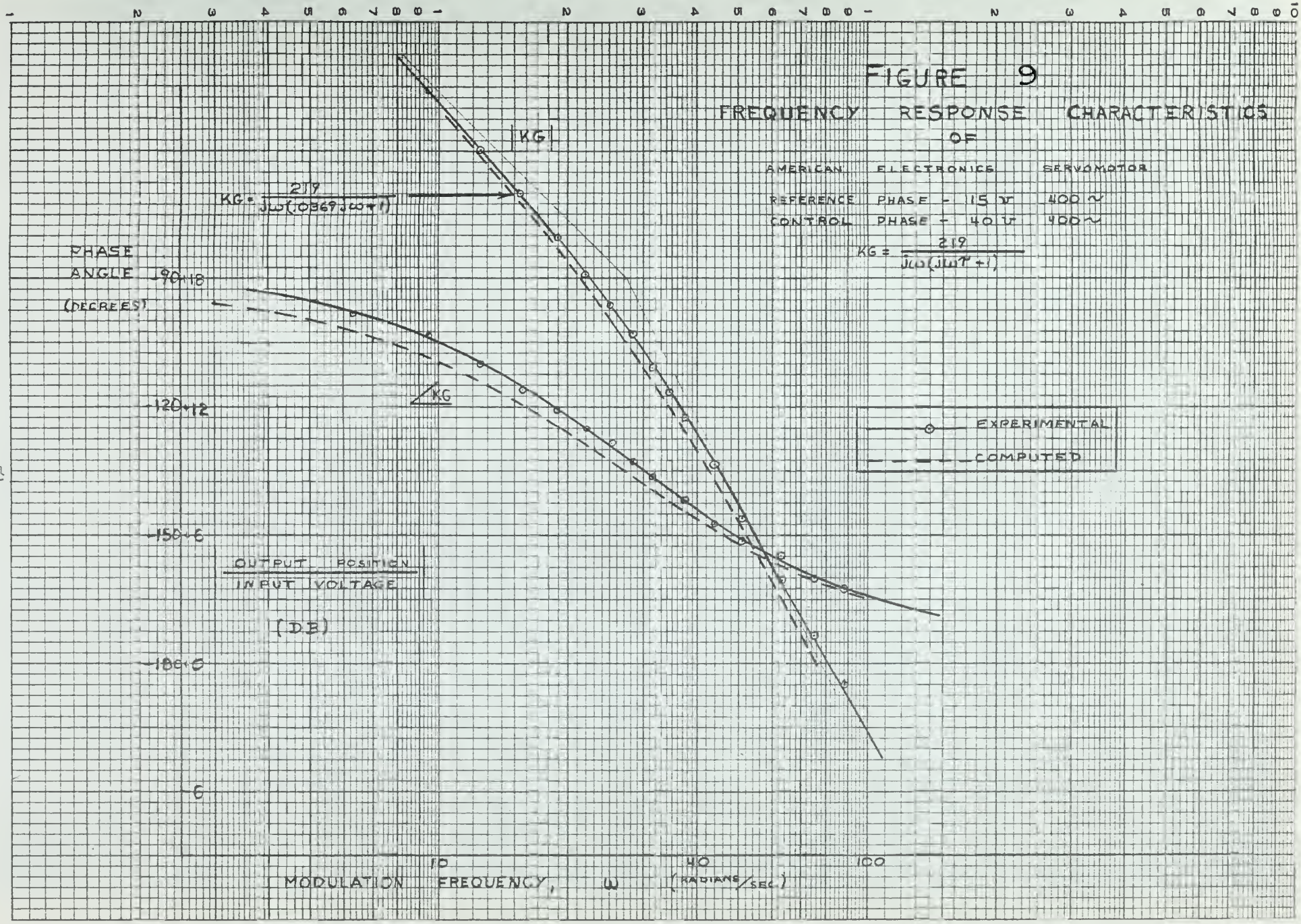
FIGURE 9
FREQUENCY RESPONSE CHARACTERISTICS
OF
AMERICAN ELECTRONICS SERVOMOTOR
REFERENCE PHASE - 15 V 400 ~
CONTROL PHASE - 40 V 400 ~
$KG = \frac{219}{j\omega(j\omega T + 1)}$
$KG = \frac{219}{j\omega(.0369 j\omega + 1)}$
|KG|
PHASE ANGLE (DEGREES)
-90 -18
-120 -12
-150 -6
-180 -0
-6
KG
EXPERIMENTAL
COMPUTED
OUTPUT POSITION / INPUT VOLTAGE (DB)
10
40
100
MODULATION FREQUENCY, ω (RADIANS/SEC.)

FIGURE 10

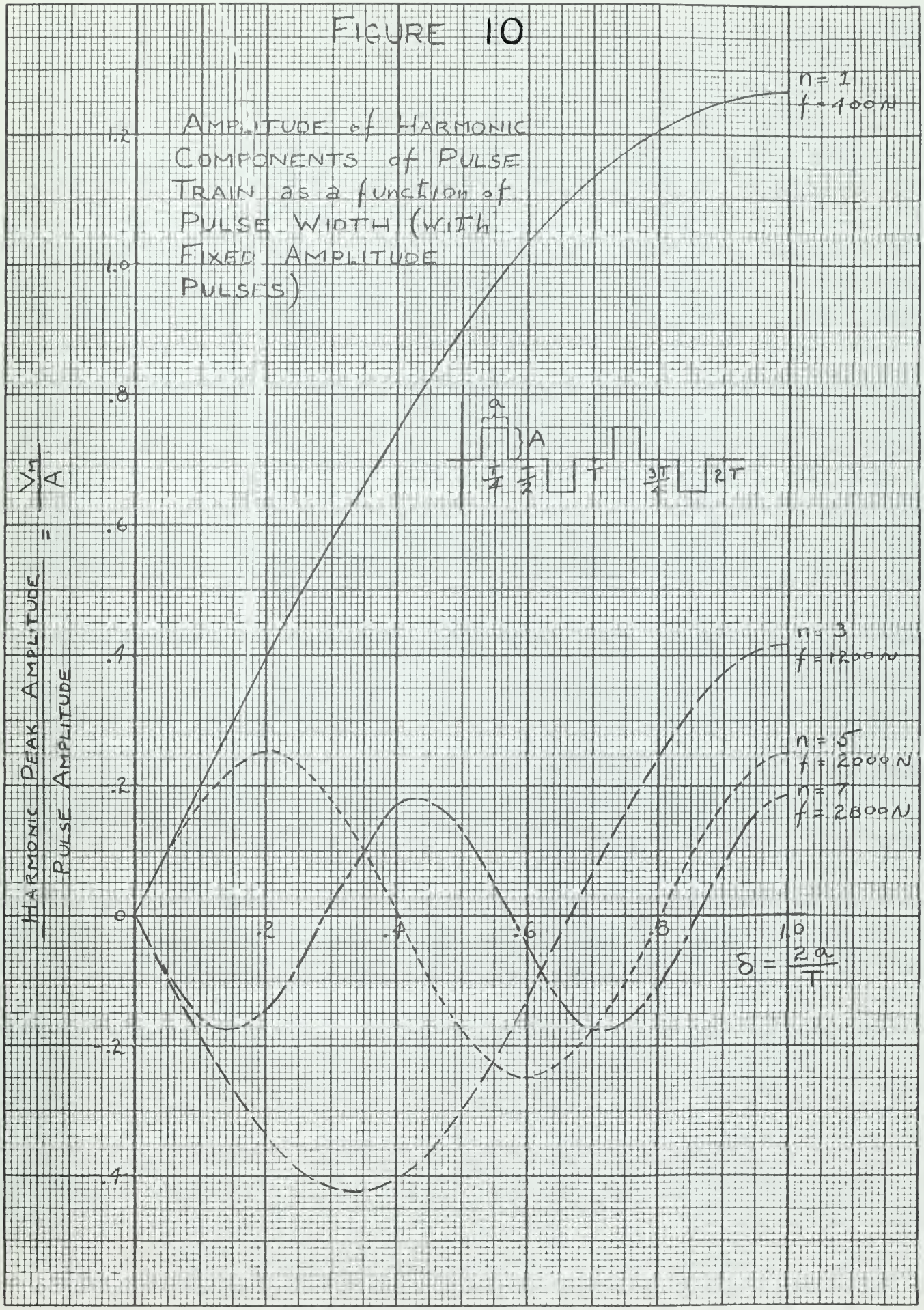
AMPLITUDE of HARMONIC COMPONENTS of PULSE TRAIN as a function of PULSE WIDTH (with FIXED AMPLITUDE PULSES)
n = 1
f = 1000N
n = 3
f = 1200N
n = 5
f = 2000N
n = 7
f = 2800N
HARMONIC PEAK AMPLITUDE / PULSE AMPLITUDE = Vn/A
δ = 2a/T
1.2
1.0
.8
.6
.4
.2
0
-.2
-.4
.2
.4
.6
.8
1.0
a
A
T/4
T/2
T
3T/2
2T

FIGURE 11

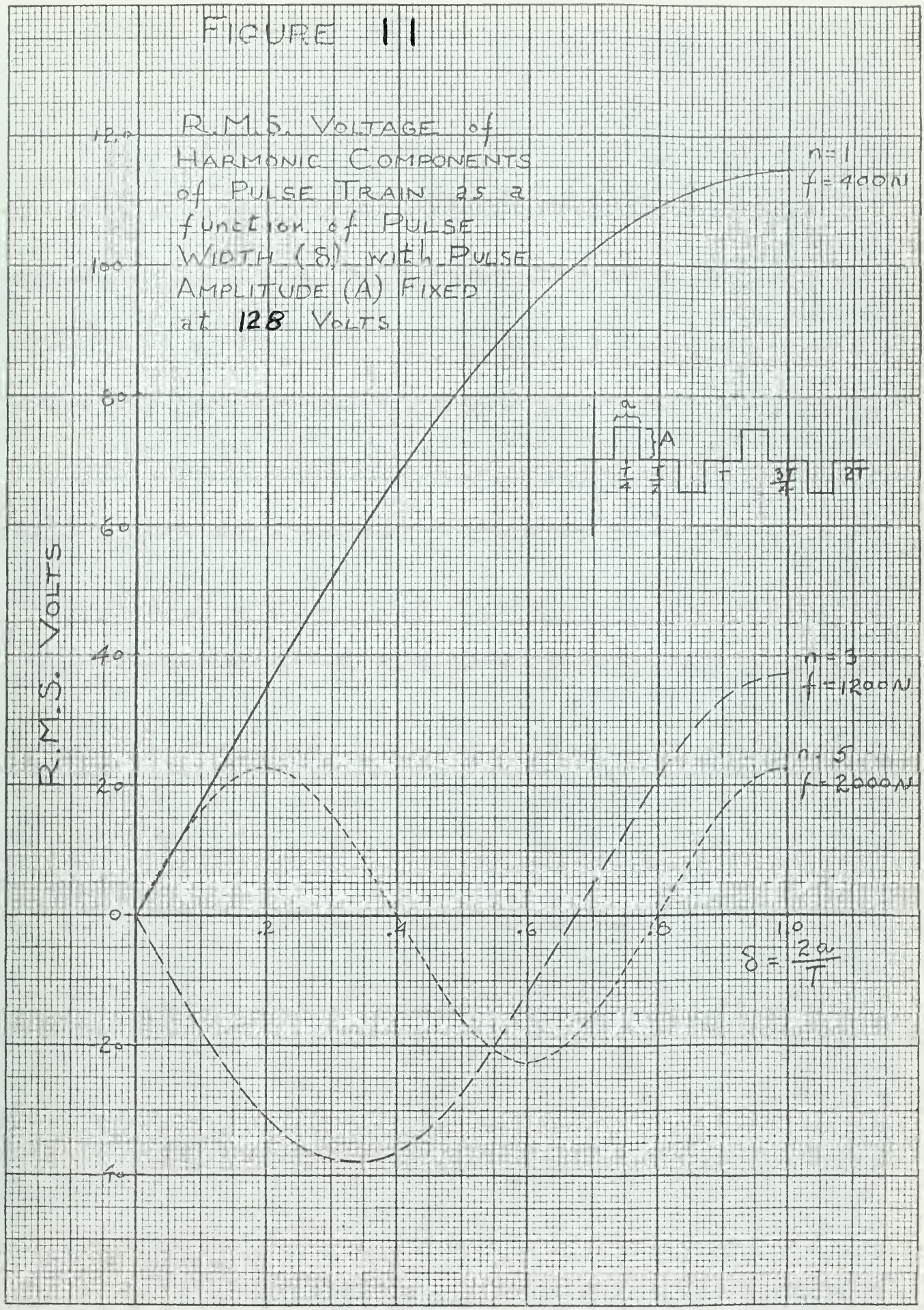
R.M.S. Voltage of Harmonic Components of Pulse Train as a function of Pulse Width (δ) with Pulse Amplitude (A) Fixed at 128 Volts
R.M.S. Volts
120
100
80
60
40
20
0
20
40
n=1
f=400N
n=3
f=1200N
n=5
f=2000N
A
a
T/4
T/2
T
3T/4
2T
.2
.4
.6
.8
1.0
δ = 2a/T

FIGURE 12

PULSE WIDTH RATIO ($\delta = \frac{2\sigma}{T}$)
and
FUNDAMENTAL PEAK AMPLITUDE
vs
TIME in PERIODS

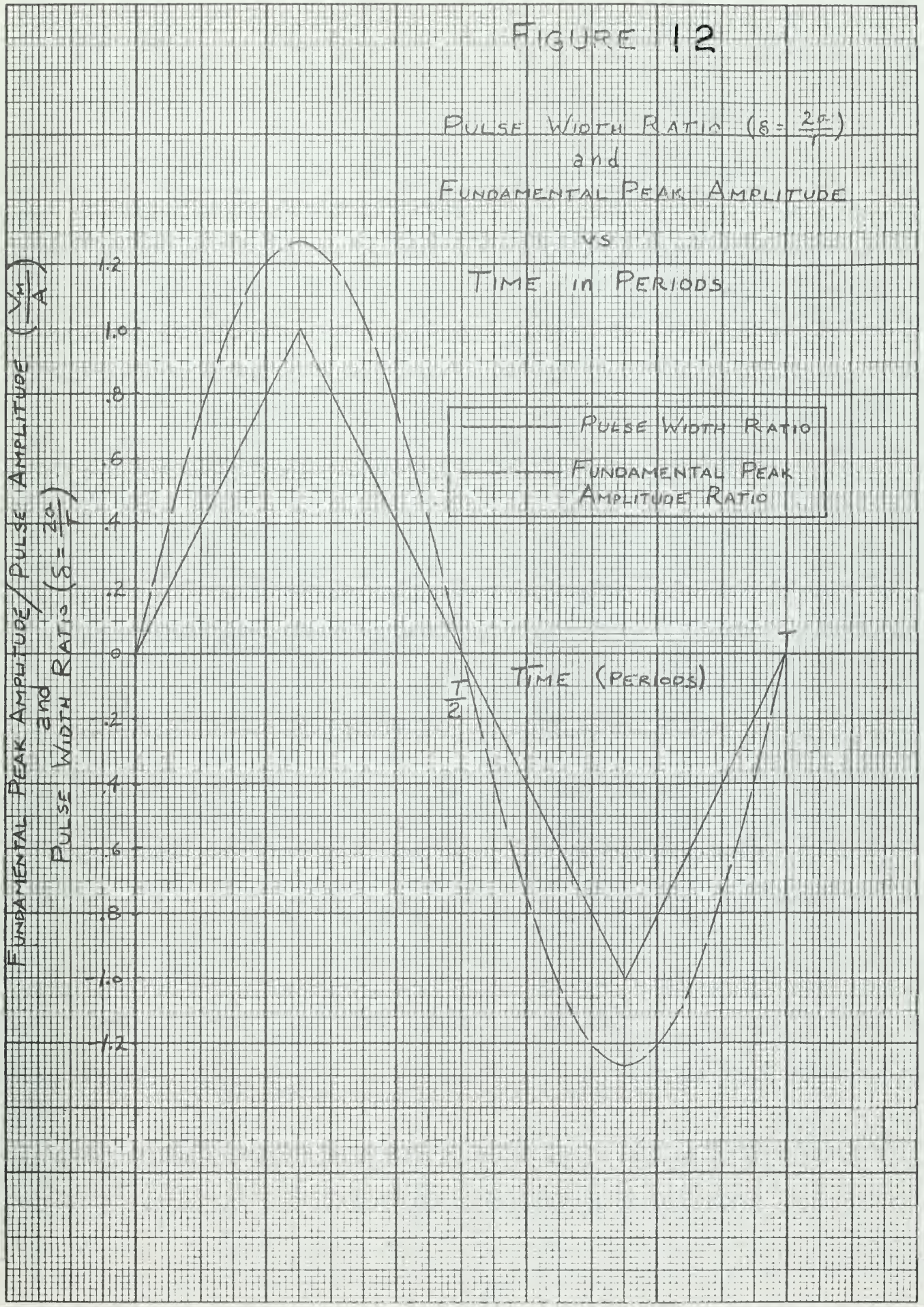

FIGURE 13

STALL TORQUE VS PULSE WIDTH

Same Excitation to Both Fields of American Electronics Servomotor

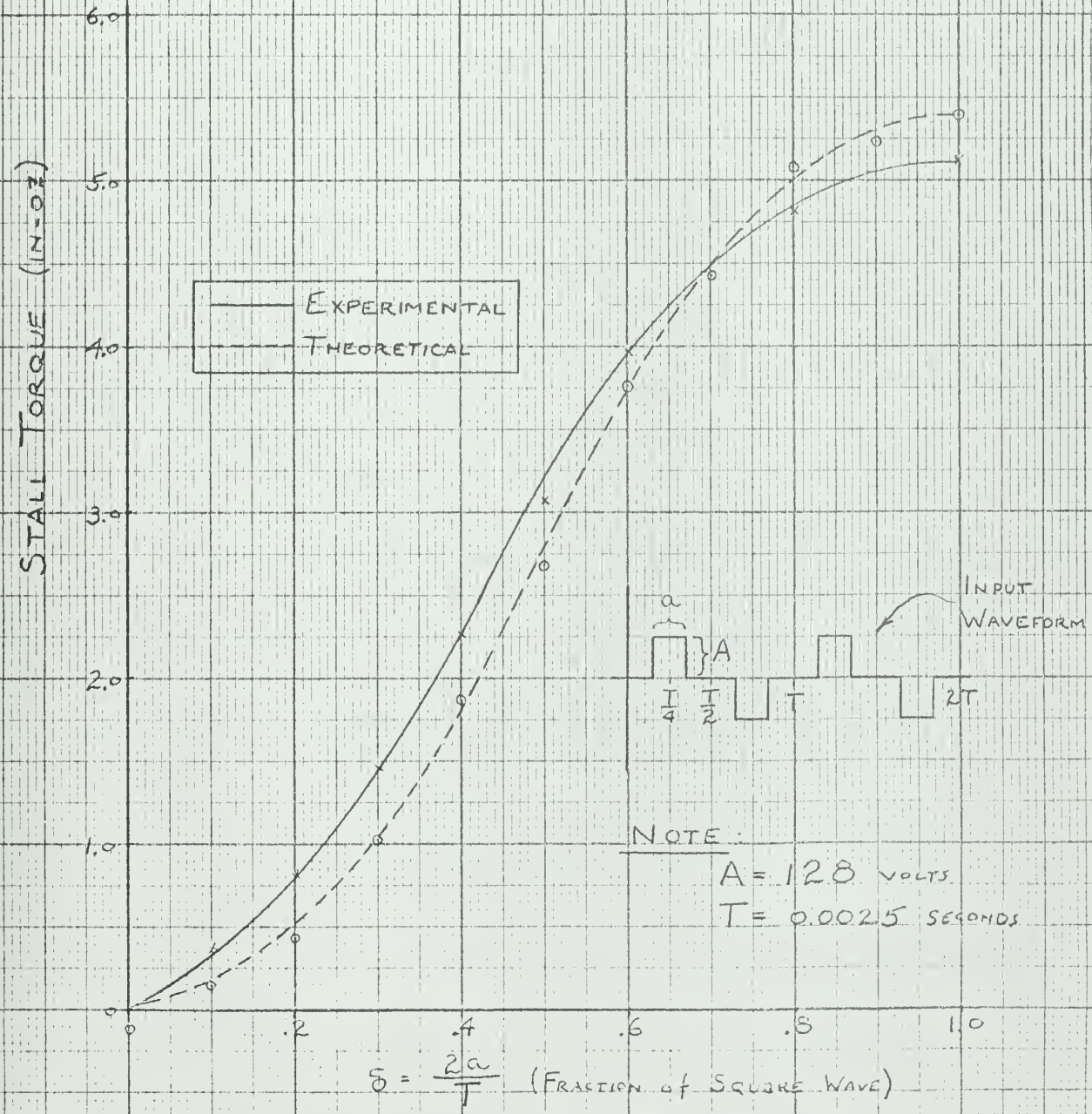

FIGURE 14

TORQUE VS SPEED

COMPARISON BETWEEN BALANCED SINE WAVE EXCITATION (EXPERIMENTAL DATA) and BALANCED PULSE EXCITATION (CALCULATED)

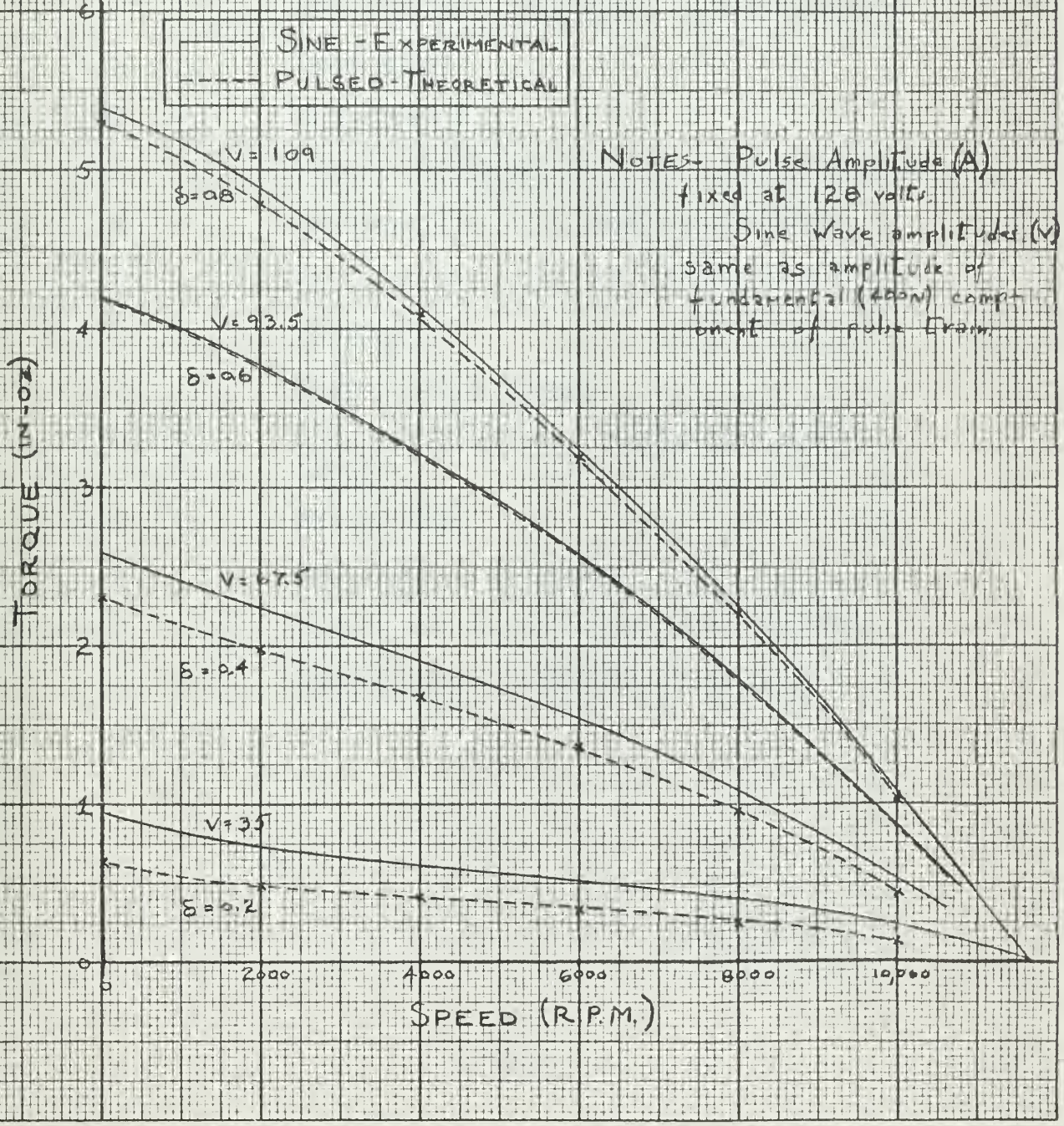

NOTES- Pulse Amplitude (A) fixed at 128 volts.
Sine Wave amplitudes (V) same as amplitude of fundamental (400N) component of pulse train.

KEY TO FIGURES 15, 21, and 24

Letter	Description
A	Pulse Modulator Unit - Amplifying and clipping circuits (4) and summing circuits (2)
B	Resolvers, Reeves type R-151
C	Drive Motor, two-phase, variable speed
D	Test motor
E	Dynamometer
F	Decade capacitor (0.1 to 1.0 microfarad)
G	McIntosh 200 watt power amplifiers
H	D.C. power supply for dynamometer brake
I	Strobotac
J	Thermocouple bridge
K	D.C. plate voltage supply for pulse former
L	Switch box
M	Tachometer, 400 cycle
N	Variac for drive motor speed control
O	Oscilloscope, TEKTRONIX type 515A

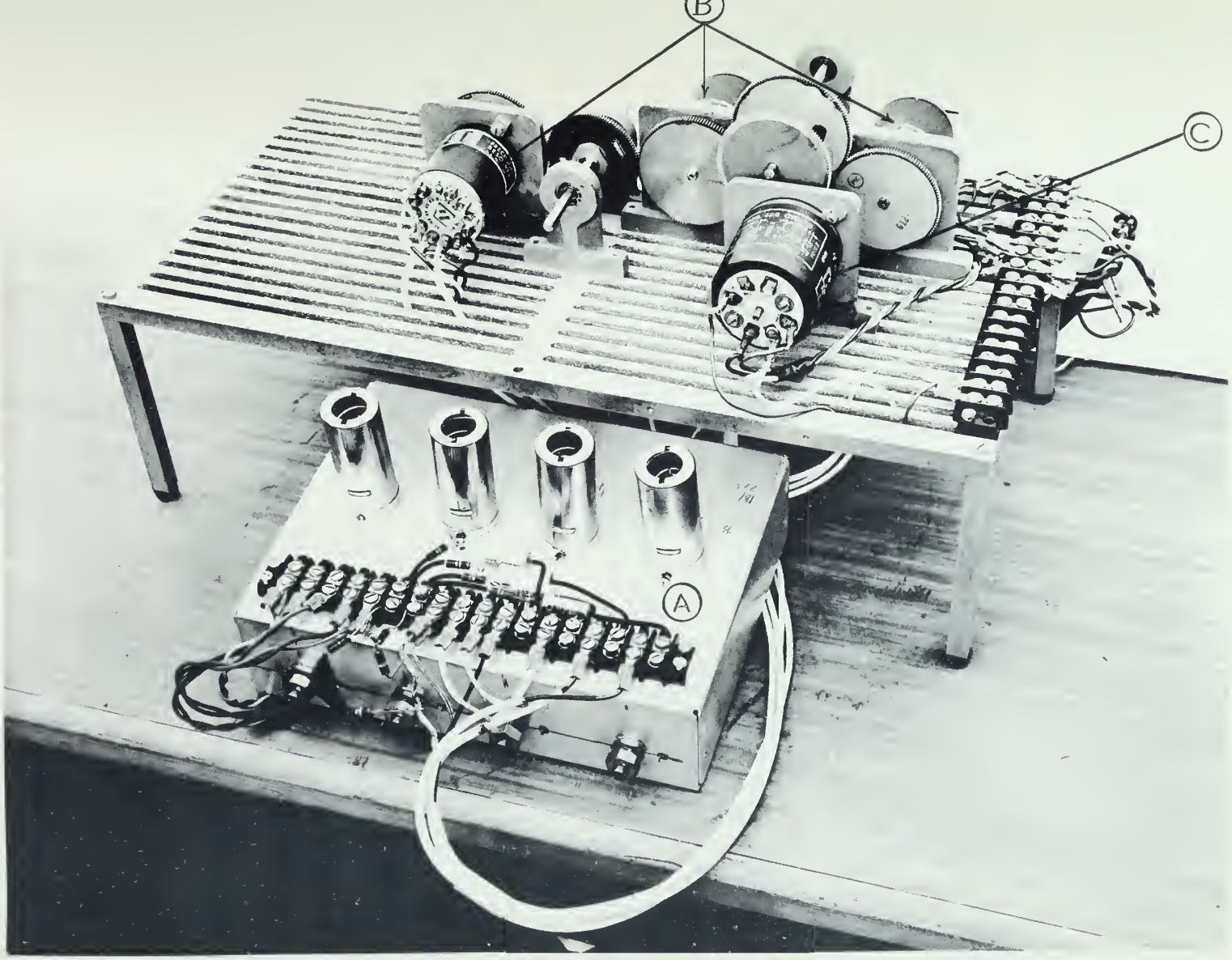

FIGURE 15 : Pulse Forming Unit

FIGURE 16

PULSE FORMING NETWORK

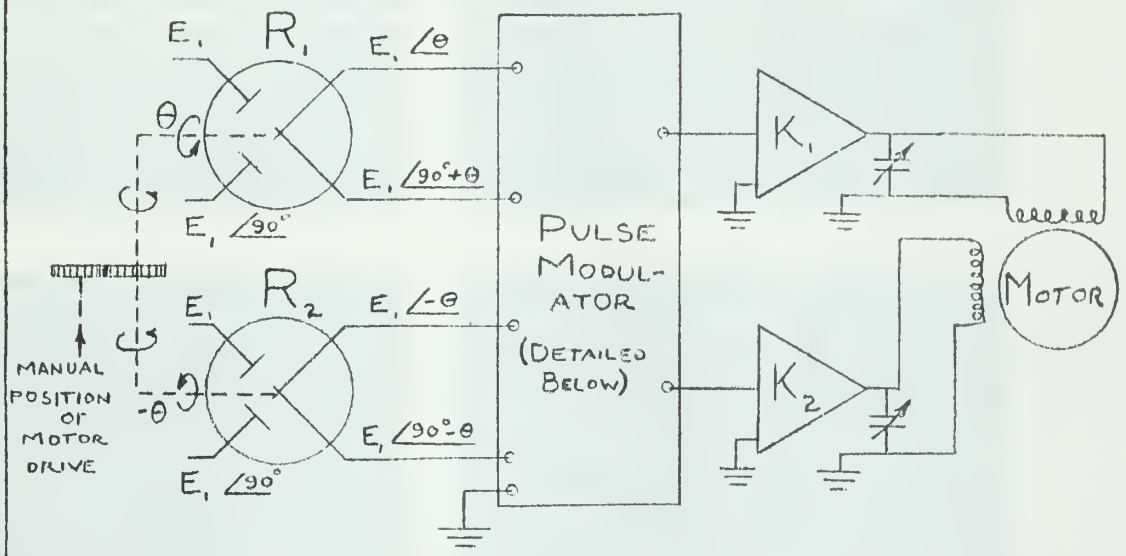

KEY -

R_1, R_2 - REEVES RESOLVERS - TYPE R 151

K_1, K_2 - M^{c}INTOSH 200 WATT POWER AMPLIFIERS

PULSE MODULATOR (1 SECTION - 2 REQUIRED)

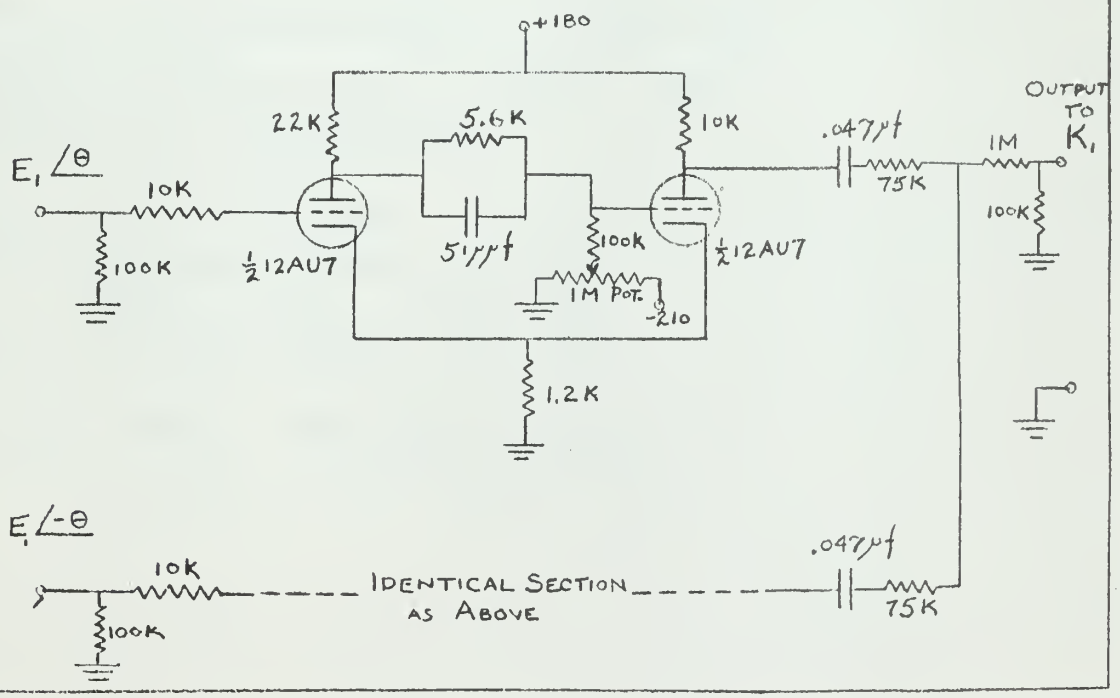

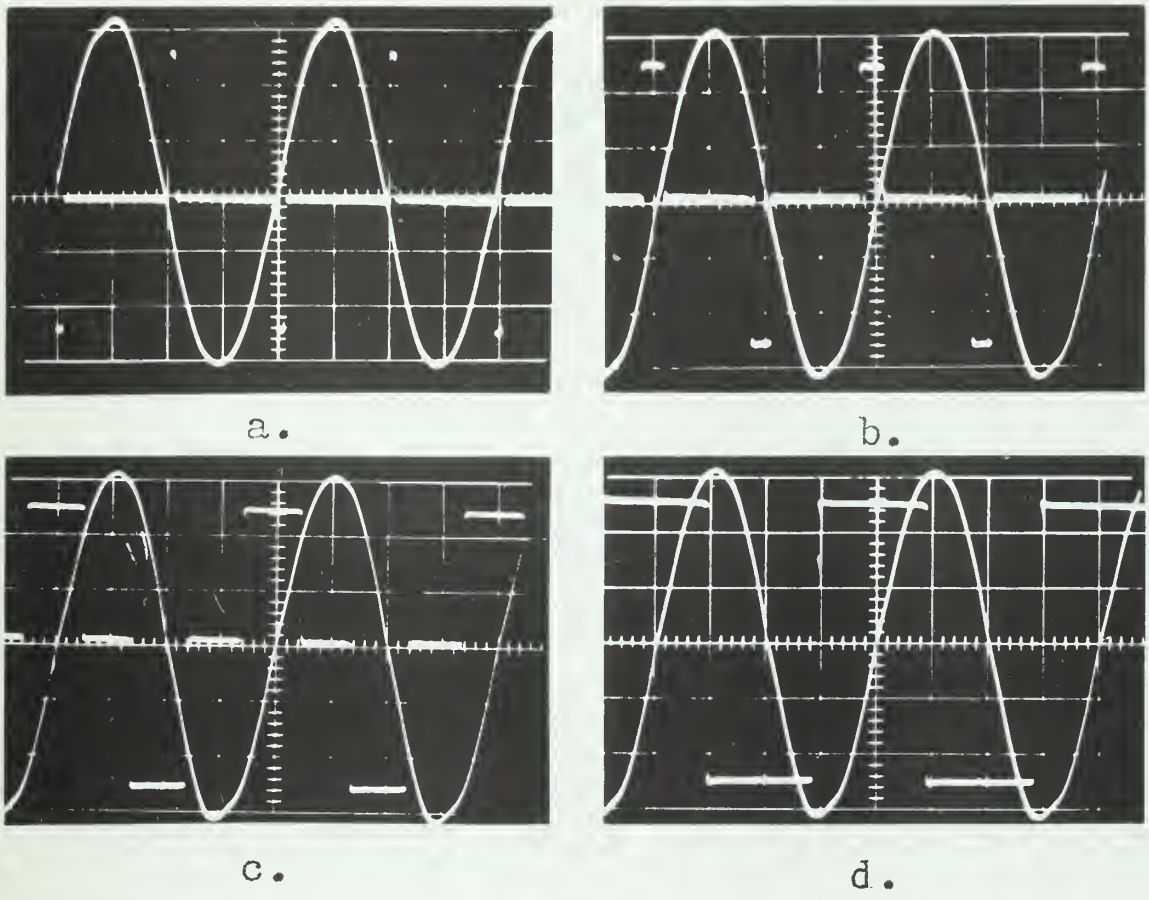

a. b. c. d.

FIGURE: 17

PULSE WIDTH MODULATED SIGNAL for Control Phase and 115 volt, 400 cycle for fixed phase.

a. spike pulse
b. narrow pulse, $\delta = 0.2$
c. 50% pulse, $\delta = 0.5$
d. square wave, $\delta = 1.0$

scale: vert. 50 volts/line
horiz. 0.625 msec/line

FIGURE 18

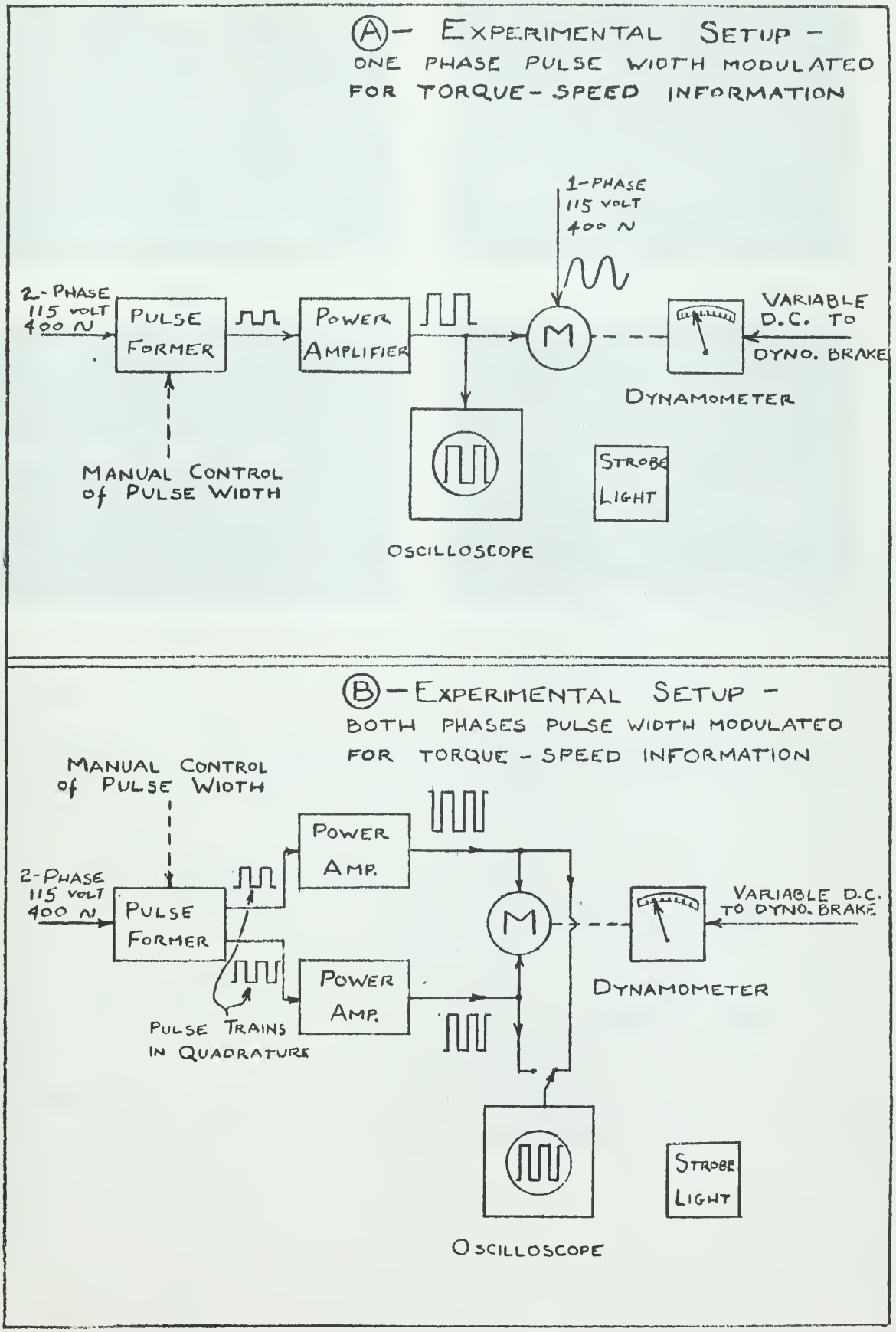
Ⓐ – EXPERIMENTAL SETUP –
ONE PHASE PULSE WIDTH MODULATED
FOR TORQUE – SPEED INFORMATION
1-PHASE
115 VOLT
400 N
2-PHASE
115 VOLT
400 N
PULSE
FORMER
POWER
AMPLIFIER
M
VARIABLE
D.C. TO
DYNO. BRAKE
DYNAMOMETER
MANUAL CONTROL
of PULSE WIDTH
STROBE
LIGHT
OSCILLOSCOPE
Ⓑ – EXPERIMENTAL SETUP –
BOTH PHASES PULSE WIDTH MODULATED
FOR TORQUE – SPEED INFORMATION
MANUAL CONTROL
of PULSE WIDTH
2-PHASE
115 VOLT
400 N
PULSE
FORMER
POWER
AMP.
POWER
AMP.
M
VARIABLE D.C.
TO DYNO. BRAKE
DYNAMOMETER
PULSE TRAINS
IN QUADRATURE
STROBE
LIGHT
OSCILLOSCOPE

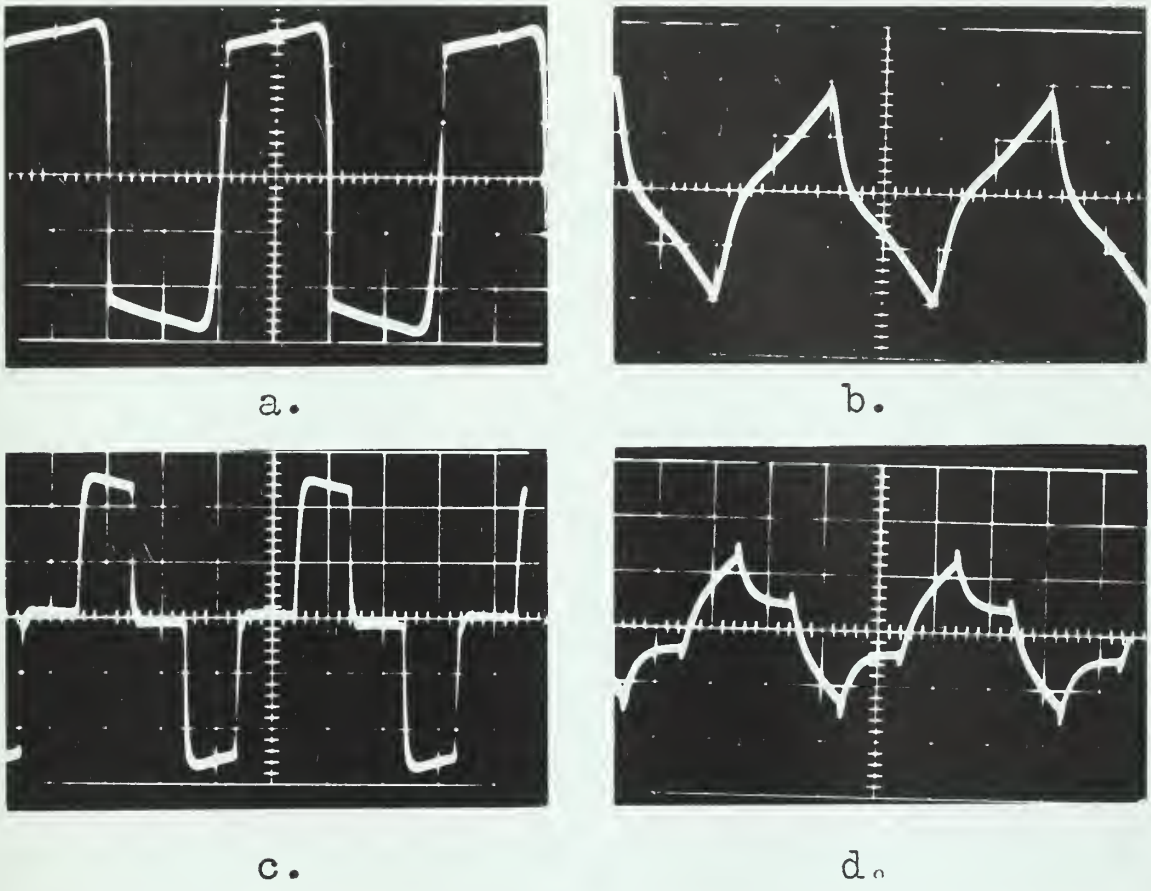

a. b.

c. d.

FIGURE 19

Voltage and current through Control Phase with Pulsed Excitation

a. square wave voltage
b. current (voltage across 1 ohm pure resistance)
c. 50% pulse voltage, = 0.5
d. current (voltage across 1 Ohm pure resistance)

scale: vert. 50 volts/line
horiz. 0.625 msec/line

FIGURE 20

TORQUE VS. SPEED

COMPARISON BETWEEN PULSE and SINE WAVE EXCITATION of CONTROL FIELD; REFERENCE FIELD FIXED.

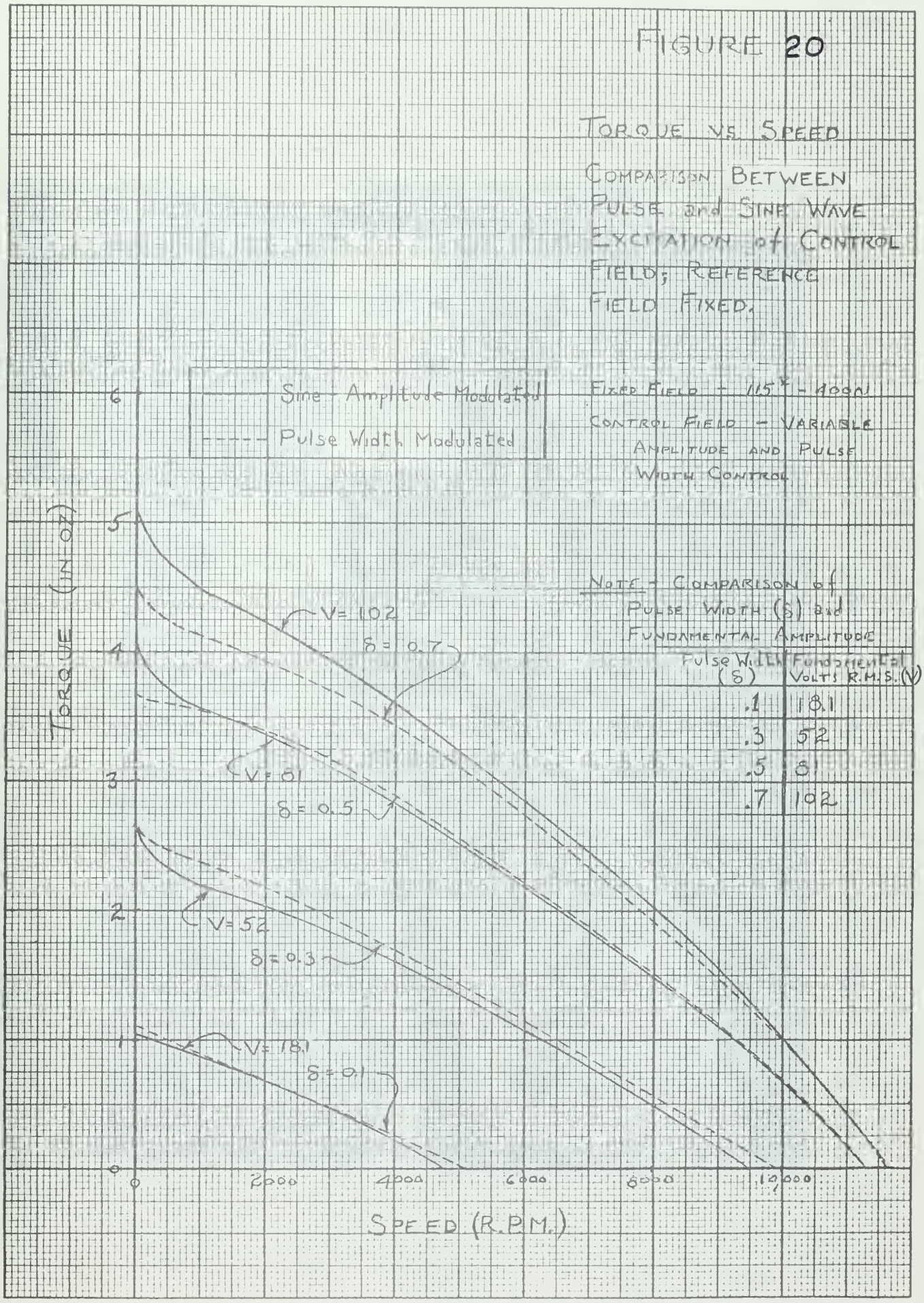

NOTE - COMPARISON of PULSE WIDTH (δ) and FUNDAMENTAL AMPLITUDE

Pulse Width (δ)	Fundamental Volts R.M.S. (V)
.1	18.1
.3	52
.5	81
.7	102

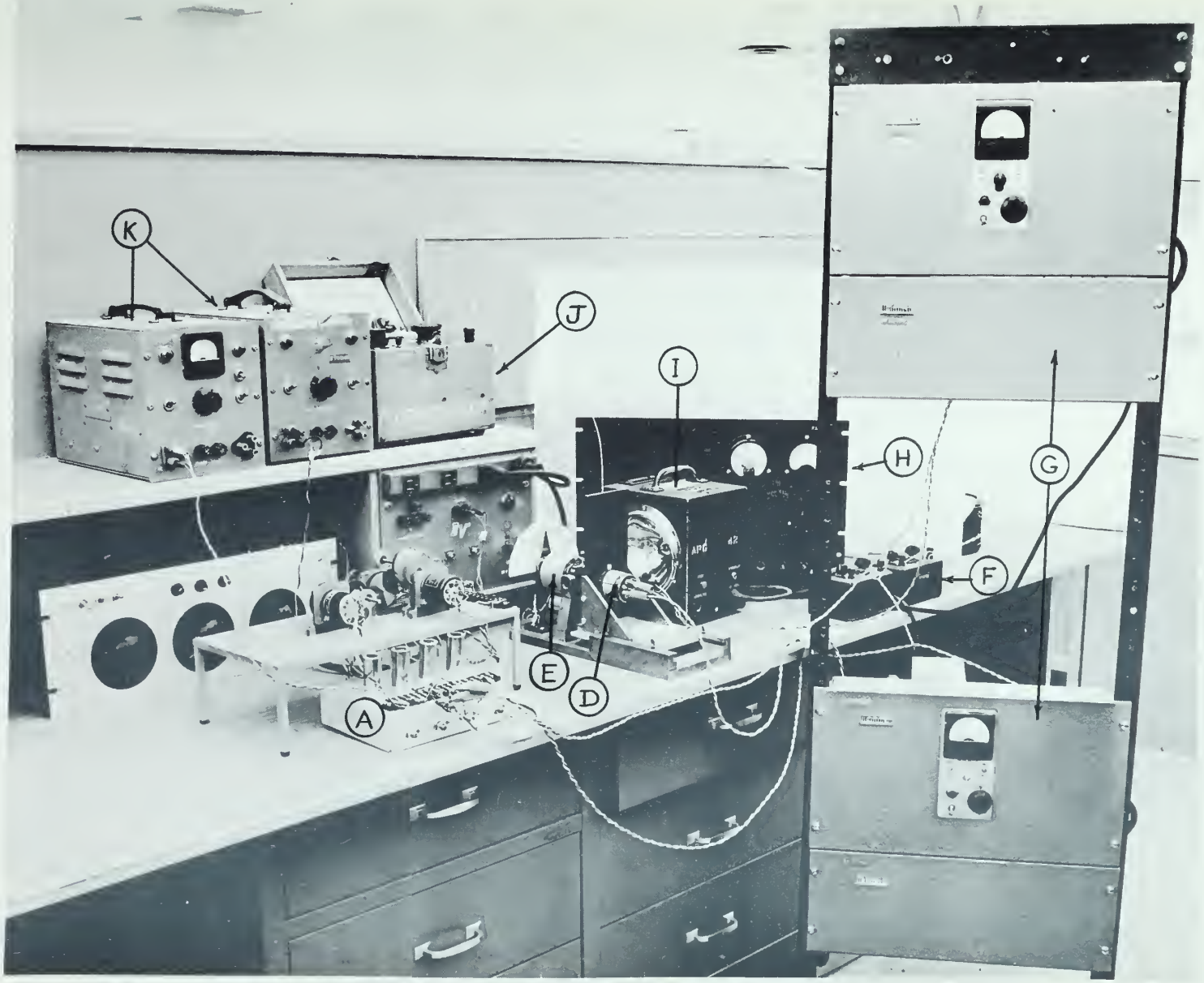

FIGURE 21: Equipment For Torque - Speed Measurements of Pulse Modulated Servomotor

FIGURE 22

TORQUE VS SPEED

COMPARISON BETWEEN PULSE and SINE WAVE EXCITATION of BOTH MOTOR FIELDS EQUALLY

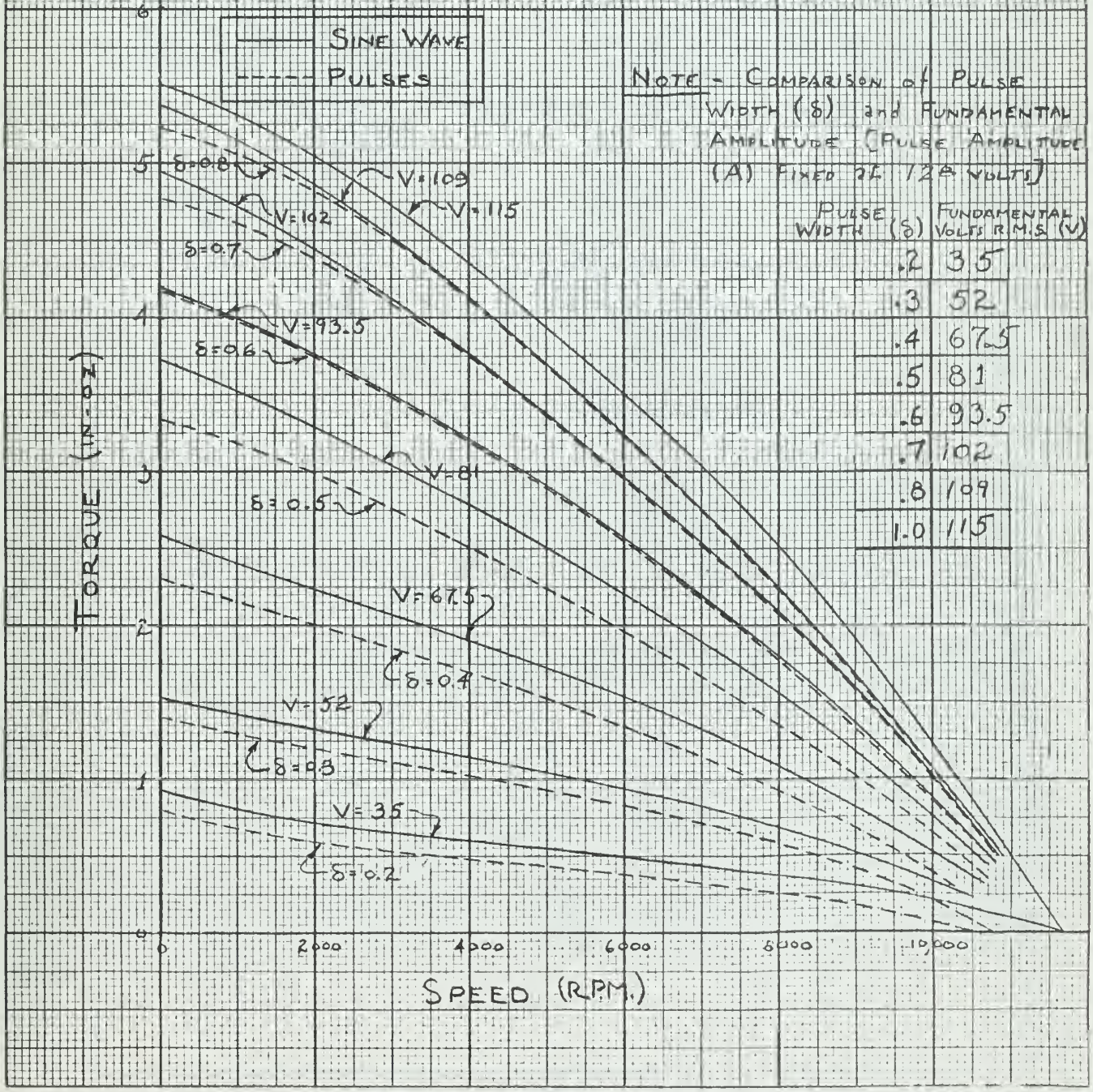

NOTE - COMPARISON of PULSE WIDTH (δ) and FUNDAMENTAL AMPLITUDE (PULSE AMPLITUDE (A) FIXED at 128 VOLTS)

PULSE WIDTH (δ)	FUNDAMENTAL VOLTS R.M.S. (V)
.2	35
.3	52
.4	67.5
.5	81
.6	93.5
.7	102
.8	109
1.0	115

FIGURE 23

EXPERIMENTAL SETUP - PERIODIC, VARIABLE FREQUENCY, PULSE WIDTH MODULATION of CONTROL PHASE for FREQUENCY RESPONSE INFORMATION

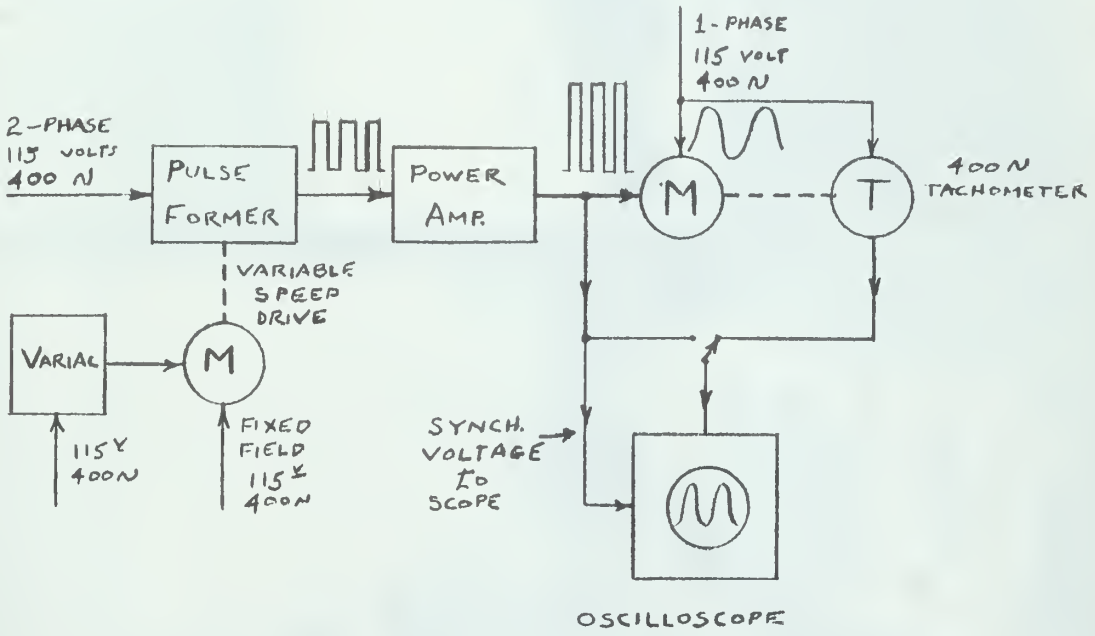

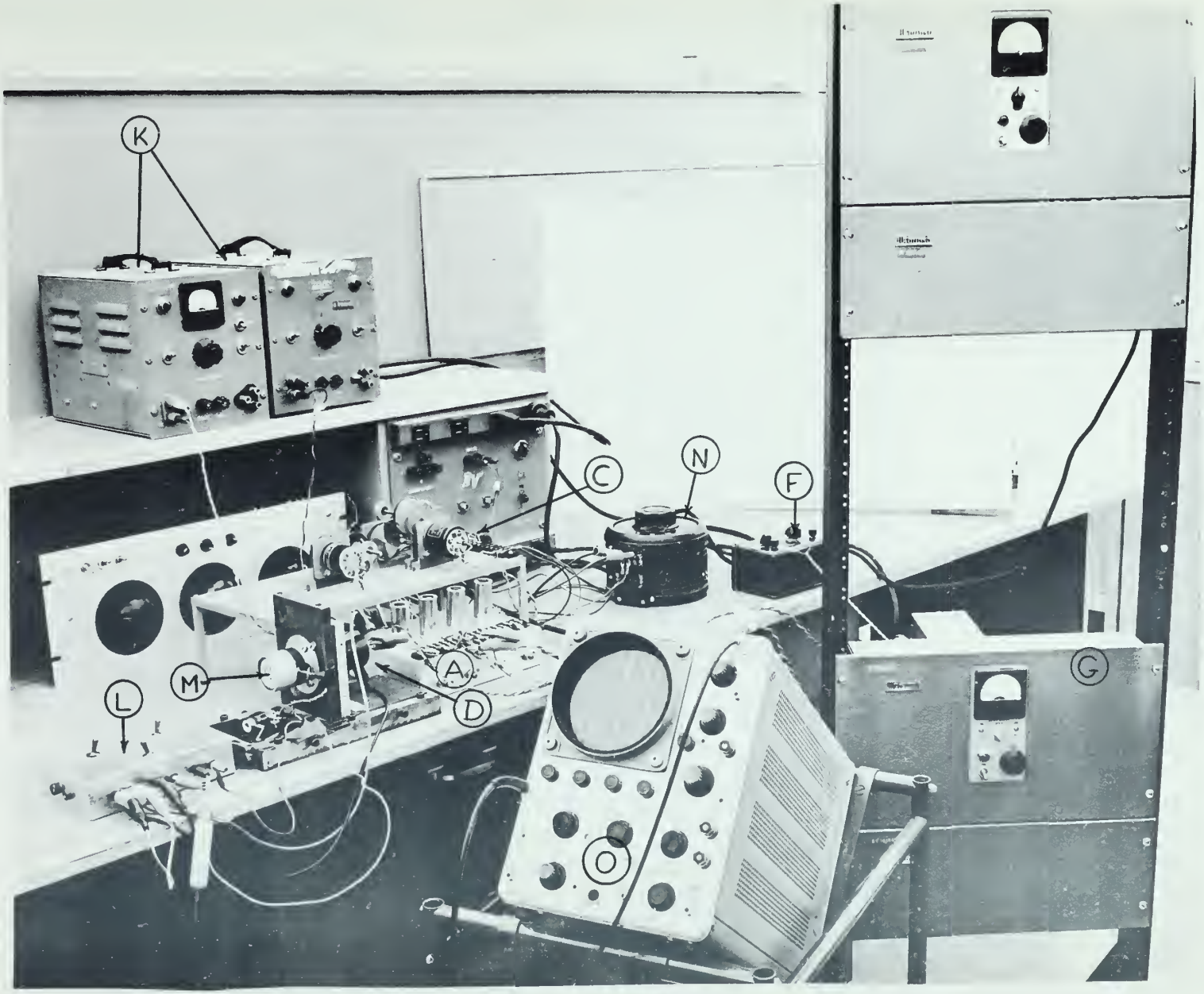

FIGURE 24: Equipment For Pulse Width Modulated Frequency Response Measurement

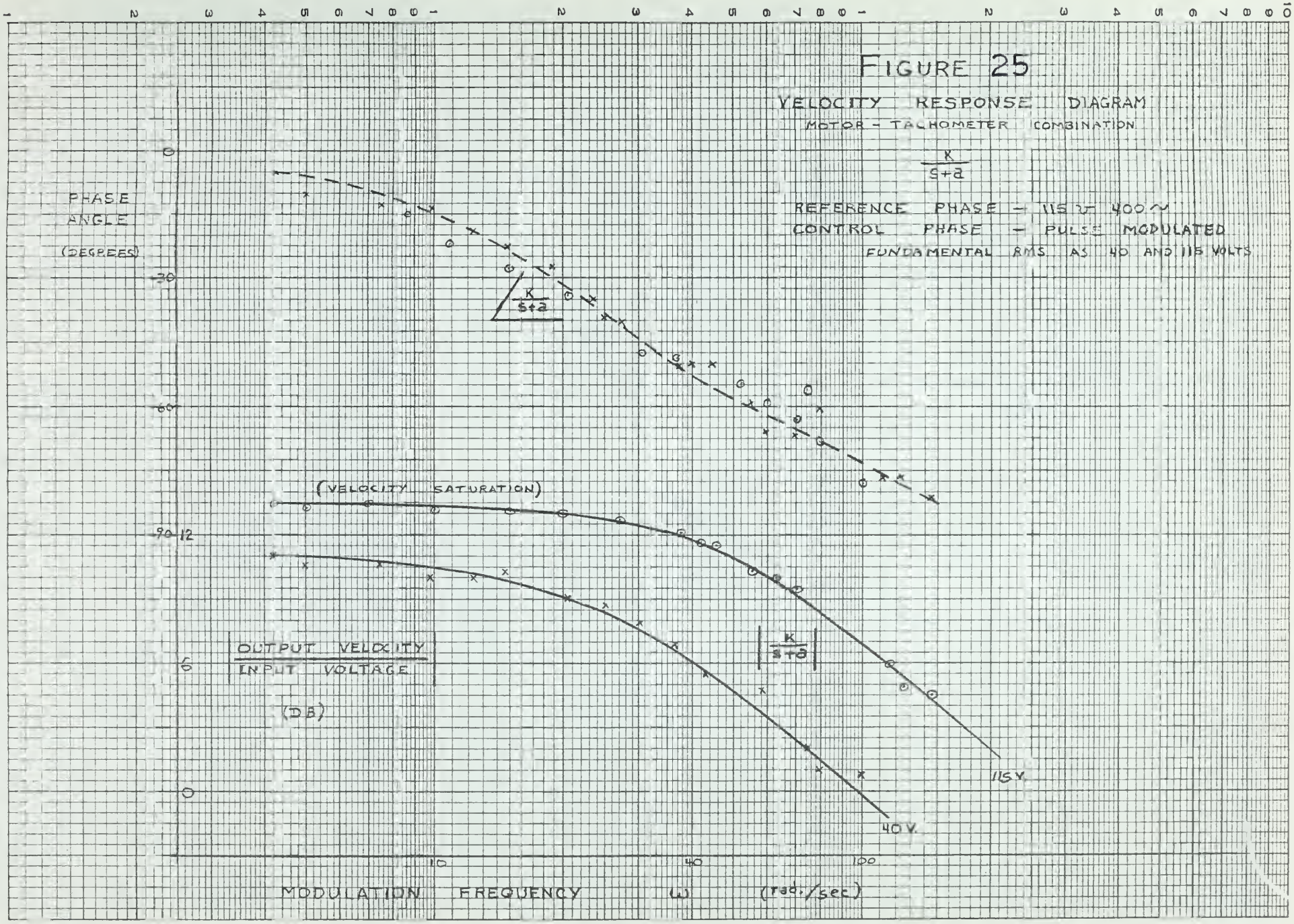
FIGURE 25
VELOCITY RESPONSE DIAGRAM
MOTOR - TACHOMETER COMBINATION
K / s+a
REFERENCE PHASE - 115 V 400 ~
CONTROL PHASE - PULSE MODULATED
FUNDAMENTAL RMS AS 40 AND 115 VOLTS
PHASE ANGLE (DEGREES)
0
-30
-60
-90
-120
(VELOCITY SATURATION)
OUTPUT VELOCITY / INPUT VOLTAGE
(DB)
|K / s+a|
115 V.
40 V.
10
40
100
MODULATION FREQUENCY ω (rad./sec.)

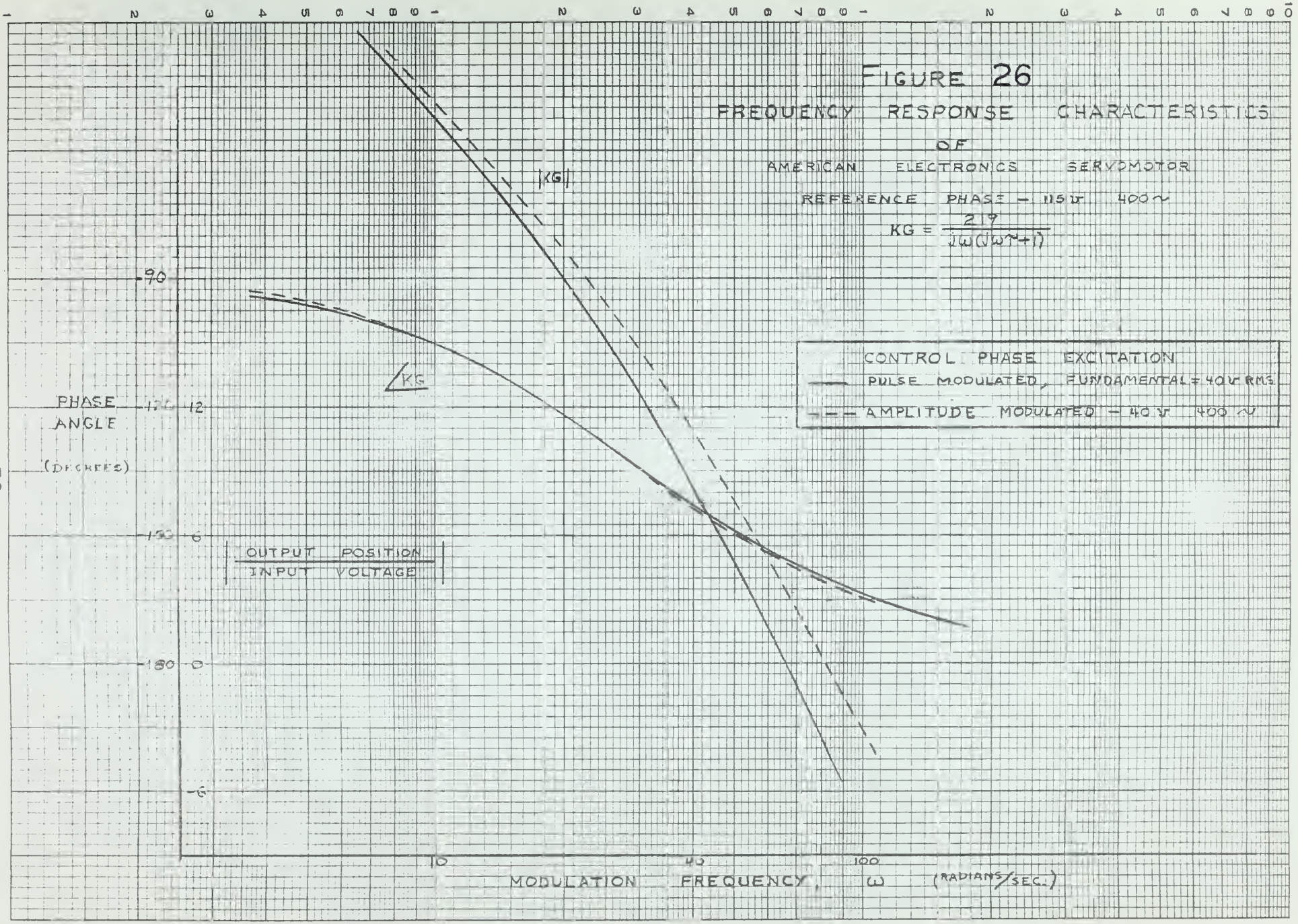
FIGURE 26
FREQUENCY RESPONSE CHARACTERISTICS
OF
AMERICAN ELECTRONICS SERVOMOTOR
REFERENCE PHASE – 115 V 400 ~
KG = 219 / Jω(Jω²+1)
|KG|
∠KG
-90
-180
12
6
0
-6
PHASE ANGLE (DEGREES)
OUTPUT POSITION / INPUT VOLTAGE
CONTROL PHASE EXCITATION
PULSE MODULATED, FUNDAMENTAL = 40 V RMS
AMPLITUDE MODULATED – 40 V 400 ~
10
40
100
MODULATION FREQUENCY, ω (RADIANS/SEC.)

FIGURE 27

STALL TEMPERATURE
FOR
AMERICAN ELECTRONICS SERVOMOTOR
MOTOR STALLED TEN MINUTES
FOR VARIOUS MODES OF EXCITATION